The ventral striatum contributes to energy balance

Roman Walle [1,*], Anna Petitbon [1], Giulia R. Fois [2], Andrea Contini [1], Rodrigue Ortole [1], Asma Oummadi [1], Véronique De Smedt-Peyrusse [1], Alban de Kerchove d'Exaerde[3], Brunos Giros [4,5], Francis Chaouloff [6], Guillaume Ferreira [1], Fabien Ducrocq [1], François Georges [2] and Pierre Trifilieff [1,*]

[1] Université de Bordeaux, INRAE, Bordeaux INP, NutriNeuro, 33000, Bordeaux, France

[2] Univ. Bordeaux, CNRS, IMN, UMR5293 F-33000 Bordeaux

[3] Laboratory of Neurophysiology, ULB Neuroscience Institute, WELBIO, Université Libre de Bruxelles (ULB), Brussels, Belgium

[4] Department of Psychiatry, Douglas Hospital, McGill University; Montreal, QC, Canada.

[5] Université de Paris Cité, INCC UMR 8002, CNRS ; F-75006 Paris, France.

[6] Endocannabinoids and NeuroAdaptation, NeuroCentre INSERM U1215, 33077 Bordeaux, France; Université de Bordeaux, 33077 Bordeaux, France

*Correspondence to Pierre Trifilieff (pierre.trifilieff@inrae.fr) or Roman Walle (roman.walle@live.fr)

Contact information: Pierre Trifilieff (Lead contact) or Roman Walle

INRAE, UMR 1286, Laboratoire NutriNeuro, Université de Bordeaux, Batiment UFR Pharmacie - 2eme Tranche - 2eme Etage – CC34, 146 rue Léo Saignat, 33076 BORDEAUX Cedex - France.

pierre.trifilieff@inra.fr; roman.walle@live.fr

Phone: +33557571248

SUMMARY

Obesity-related pathologies and anorexia nervosa are increasingly considered as opposite ends of eating disorders (ED) spectrum. Accordingly, accumulating evidence points to opposite dysregulations of common brain systems in these pathologies, the Nucleus Accumbens (NAc) in particular. However, to which extent alterations in NAc activity are sufficient to elicit ED-like behavioral dimensions remains to be established. Using acute, bidirectional, chemogenetic modulation of each NAc medium spiny neuron (MSN) subpopulation, we found that D1-MSNs and D2-MSNs oppositely regulate the balance between food intake and exercise-induced energy expenditure. As opposed to the limited effect of repeated chemogenetic manipulations of each MSN subpopulation, the concomitant manipulation of both MSN subpopulation had sustained effects. Repeated activation of D1-MSNs combined with repeated inhibition of D2-MSNs biased behavior toward activity-related energy expenditure leading to weight/fat loss, whilst the opposite manipulations favored energy intake and hence weight/fat gain. These results suggest that dysregulations of NAc dopaminoceptive MSN network might be at the core of EDs.

Keywords: Eating disorders, energy balance, motivation, nucleus accumbens, medium spiny neurons, chemogenetics

INTRODUCTION

Overeating/obesity-related pathologies and anorexia nervosa (AN) are multifactorial diseases resulting from an interaction between genetic and environmental factors. They can be considered as extreme two ends of the spectrum of eating disorders (EDs), wherein psychiatric symptoms are coupled to metabolic alterations, making them increasingly viewed as “metabo-psychiatric” diseases (Watson et al., 2019; Weiss et al., 2020). Such a continuum in ED subtypes is supported by genome-wide association studies (GWAS) revealing an inverse genetic correlation between AN and obesity (Bulik-Sullivan et al., 2015), as well as overlapping environmental factors (Krug et al., 2013). Dimensional approaches through the RDoC framework to EDs reveals alterations in common domains such as negative (stress, anxiety) and positive (motivation, reward processing) valence systems (Wildes and Marcus, 2015). In particular, beyond the opposite feeding pattern, which might be related to inverse alterations of food-related reward valuation (Wildes and Marcus, 2015), reward processing tends to be dysregulated in opposite manners in overeating and AN. In particular, an increased drive to exercise due to an enhanced reinforcing value of physical activity is a typical feature of AN that persists after remission and might even precede the development of the disease (Casper, 2018; Klein et al., 2010; Shroff et al., 2006; Taranis and Meyer, 2011). On the other hand, obesity is associated to physical hypoactivity even after recovery (Matikainen-Ankney and Kravitz, 2018). These differential alterations of physical activity in EDs have been proposed to be linked to the rewarding impact of exercise and/or the motivation to engage in physical activity (Rizk et al., 2020; Ruegsegger and Booth, 2017). Such overlapping symptomatic dimensions in EDs suggest opposite dysfunctions within common brain networks, especially the reward system.

In regard to its well-established role in reward processing, motivation and locomotor activity, the nucleus accumbens (NAc) has received particular attention as it stands as a hub within the reward system, computing sensory, cognitive and reward information to modulate goal-directed behaviors (Floresco, 2015). Functional imaging reveals that NAc activity is regulated in opposite manner in AN and obese subjects in response to food cues (Frank et al., 2012). Hence, this suggests that the reward system is hyperresponsive in AN while hyporesponsive in obese subjects (Kaye et al., 2013), at least in relation to food-related stimuli. In the same vein, studies aiming at addressing the integrity of dopamine transmission found decreased and increased striatal dopaminergic D2/3 receptor binding in obese subjects (Volkow et al., 2008; Wang et al., 2001) and in AN individuals (Bailer et al., 2013; Frank et al., 2012), respectively. Even though these latter imaging data are controversial (Broft et al., 2015; Dang et al., 2016; Gaiser et al., 2016; Karlsson et al., 2015), animal studies tend to support a main implication of striatal D2-dependent transmission in EDs. In fact, downregulation of striatal D2 receptor leads

to compulsion towards palatable food (Johnson and Kenny, 2010). Conversely, its overexpression in the NAc induces rapid weight loss in female mice exposed to the so-called activity-based anorexia (ABA) model, which involves food access restriction (Welch et al., 2019). Interestingly, such effects of manipulations of D2 receptor expression mainly result from physical activity-related energy expenditure rather than from a direct effect on food intake (Beeler et al., 2016; Friend et al., 2017; Welch et al., 2019).

Altogether, these findings point to D2 receptor-expressing neurons of the striatum – and the NAc in particular – playing a key role in the pathophysiology of EDs. In the NAc, the vast majority of neurons is accounted for by dopaminoceptive medium spiny neurons (MSNs) which are equally divided in two subpopulations expressing either D1 (D1-MSNs) or D2 (D2-MSNs) receptors. The respective role of D1- and D2-MSNs of the NAc have been the subject of extensive investigation for their implication in food-related reward processing and motivational processes (Carvalho Poyraz et al., 2016; Gallo et al., 2018; Natsubori et al., 2017; Soares-Cunha et al., 2016, 2018, 2020, 2022) and more recently in the regulation of food intake (Bond et al., 2020; O'Connor et al., 2015; Thoeni et al., 2020; Zhu et al., 2016). However, to which extent bidirectional dysregulation of MSNs activity could be sufficient to mimic specific obesity- or AN-related dimensions still remains unknown.

To solve this issue, we used a chemogenetic approach to manipulate individual subpopulations of NAc MSNs. We first found that inhibiting NAc MSNs acutely blunts (D1-MSNs) or facilitate (D2-MSNs) the willingness to exert an effort for palatable food. However, we also unraveled that whilst D1-MSNs exert strong satietogenic effects, D2-MSNs display an orexigenic control over both regular and palatable food. Such effects were accompanied by opposite influence on voluntary physical activity. Upon chronic manipulation, either D1-MSNs inhibition or D2-MSNs activation resulted in weight/fat gain, mostly due to physical hypoactivity. On the other hand, repeated activation of D1-MSNs increased physical activity and food consumption (despite an initial decrease in food intake) which led to the maintenance of energy balance. When MSNs were concomitantly manipulated, inhibition of D1-MSNs together with activation of D2-MSNs led to an obesity-like phenotype which was mostly related to a decrease in exercise-mediated energy expenditure. Conversely, chronic activation of D1-MSNs together with D2-MSNs inhibition led to an AN-like phenotype, translating in an exaggerated physical activity not fully compensated by food intake. Altogether, these findings point to NAc MSNs network being at the crossroad between reward processing and energy balance, further suggesting that dysfunction of that network could be a main player in ED etiology.

RESULTS

Chemogenetic activation of D1- and D2-MSNs of the NAc core have opposite effects on the firing of VTA dopamine neurons

We expressed the Cre-dependent excitatory DREADD HM3Dq fused to the red fluorescent reporter mCherry in D1- or D2-MSNs of the NAc core through local injection of adeno-associated viral vectors (AAV) in DrD2-cre or DrD1-cre mice (Figure 1). In accordance with the literature (Baimel et al., 2019; Kupchik et al., 2015; Pardo-Garcia et al., 2019), D2-MSNs exclusively project to the ventral pallidum (VP), while D1-MSNs of the NAc core project to both the VP and the SNc/VTA (Figure 1 A, C; SF1). To characterize the functional consequences of D1- or D2-MSNs activation, we recorded the activity of dopaminergic (DA) neurons of the VTA in anesthetized animals. We found that D2- and D1-MSNs activation increased and decreased firing activity of VTA-DA neurons, respectively (Figure 1 B, D). These findings are in accordance with D2-MSNs positively regulating VTA-DA neurons activity through inhibition of VP projections to the VTA (Soares-Cunha et al., 2018), while D1-MSNs of the NAc core exert an inhibitory control over VTA-DA neurons through their direct inhibitory projection to the VTA (Beier et al., 2015).

D1-MSNs and D2-MSNs of the NAc core respectively facilitate and diminish incentive processes towards palatable food

The antagonistic effects of D1- and D2-MSNs of the NAc in the modulation of motivational processes in the context of food-seeking behavior have been recently challenged. Here, we found that chemogenetic activation or inhibition of D2-MSNs did not impact licking patterns during consumption of a palatable solution (SF2), a proxy for hedonic reactivity (Johnson, 2018a; Ducrocq et al., 2019, 2020), but decreased and increased performance in a progressive ratio task, respectively (Figure 2A-D; SF2), without alteration in motoric abilities (Figure 2E, SF2), supporting an “amotivational” effect of D2-MSNs of the NAc core.

Similarly, chemogenetic manipulations of D1-MSNs spared hedonic reactivity (SF2). Regarding reward processing, inhibition of D1-MSNs decreased performance in the progressive ratio task (SF2), in accordance with their pro-motivational role. However, surprisingly, chemogenetic activation of D1-MSNs led to a comparable decrease in lever presses and breakpoint (SF2). This was accompanied by an inability to increase press rate as a function of ratio requirement in the progressive ratio task (SF2). Decreasing the dose of CNO recapitulated the blunted performance under D1-MSNs inhibition that was previously observed with higher dose of CNO (Figure 2F-H). Similarly, despite spared abilities to maintain press rate as a function of increasing ratio requirement (Figure 2I), activation of D1-MSNs still

resulted in decreased performance in the progressive ratio task (Figure 2F-H). Considering the previously described satietogenic effect of NAc shell D1-MSNs activation (Bond et al., 2020; O'Connor et al., 2015), we hypothesized that the diminution of lever pressing in our conditions could be related to a decreased hunger drive rather than blunted motivational performance *per se*.

NAc D1-MSNs and D2-MSNs exert opposite effects on food consumption

In keeping with this hypothesis, we assessed the effects of modulating MSNs activity on *ad libitum* food consumption (Figure 3A). Inhibition of D2-MSNs acutely decreased chow consumption, hence resulting in lower cumulative food intake over 48 hours (Figure 3B). D2-MSNs activation had the opposite effect, though the increased chow consumption was delayed (Figure 3C). Such effects on food intake resulted in a significant weight loss for D2-MSNs inhibition and weight gain for D2-MSNs activation, these being maintained for 48 hours (Figure 3D). Of note, these effects were not related to differences in peripheral glucose tolerance (SF3). Manipulation of D1-MSNs activity resulted in opposite findings with their inhibition leading to acute increased food intake whilst their activation strongly decreased it (Figure 3 E, F), with no effect on glucose metabolism (SF3). However, these acute effects on food intake were not accompanied by significant changes in weight at 24 or 48 hours (Figure 3G).

As food intake and willingness to work for a food reward were regulated in opposite manners by MSN manipulations, we next aimed at determining whether an increase in the motivational valence of food might lead to different outcomes on food intake. We therefore challenged mice in a fasting/refeeding protocol wherein animals were allowed access to palatable food (high-fat) after an overnight fasting (SF3). We found effects comparable to those measured during *ad libitum* chow intake, i.e. D2-MSNs inhibition decreased food intake while their activation had a delayed orexigenic effect (SF3). Manipulation of D1-MSNs triggered the opposite effects (SF3). Both high (2 mg/kg) and low (0.5 mg/kg) doses of CNO resulted in similar outcomes, with milder effects at 0.5 mg/kg. We therefore kept CNO at the dose of 2 mg/kg for the following experiments.

The effects of acute chemogenetic NAc MSN manipulations on food intake occur at the expense of voluntary physical activity

As mentioned above, alterations in voluntary physical activity are typical symptoms of EDs that go in opposite directions with food consumption. We therefore performed a choice protocol in which fasted mice had free access to food and a running wheel (Figure 4A). The acute satietogenic effect of D2-MSNs inhibition was accompanied by increased wheel running distance, while activation of D2-MSNs resulted in a strong decrease in physical activity with no

significant effect on food intake, in accordance with the delayed effect of such manipulation on feeding (Figure 4B ; SF4). In opposite, inhibition of D1-MSNs increased and decreased food intake and wheel running, respectively, while the strong satietogenic effect of D1-MSNs activation was accompanied by increased wheel running (Figure 4C ; SF4).

Chronic activation of NAc D2-MSNs leads to increased fat mass related to decreased voluntary physical activity

Altogether, our findings suggest that the opposite effects of D1- and D2-MSNs manipulation on food intake do not reflect alterations of reward processing *per se*, but could rather correspond to an imbalance between energy supply and physical activity-mediated expenditure, which is a typical feature of EDs (Lowe, 2020). Therefore, we next asked whether repeatedly manipulating MSNs activity could be sufficient for the development of some obesity- or AN-like phenotypes. To do so, mice were housed individually with free access to palatable (high fat) diet and a running wheel in order to evaluate the relative preference between the two rewards. CNO was administered every day at the onset of the dark period (Figure 5A).

Chronic D2-MSNs activation (D2 Gq) transiently increased food consumption (Figure 5B). This was accompanied by decreased voluntary wheel running throughout the entire period of CNO activation compared to controls (Figure 5C). These resulted in a significantly higher gain of fat mass measured at the end of the chronic CNO period (Figure 5D, SF5). Importantly, cessation of CNO administration led to an immediate reversion of voluntary physical activity, together with a significant decrease in food consumption (Figure 5B-C), resulting in significant weight and fat mass loss compared to controls (Figure 5D, SF5). Despite the acute increase in wheel running and decrease in food consumption, as previously found (Figure 4), animals subjected to chronic inhibition of D2-MSNs (D2 Gi) did not significantly differ from controls for any of the main variables measured (Figure 5B-D, SF5).

Enhanced voluntary wheel running under chronic activation of D1-MSNs is compensated by increased food consumption

Despite the strong satietogenic effect of D1-MSNs activation (D1 Gq) the very first day of CNO administration, the higher voluntary physical activity that was maintained across chronic D1-MSNs activation was accompanied by higher food consumption during the entire period of CNO administration compared to controls (Figure 5E, F). As a consequence, animals with chronic activation of D1-MSNs did not differ from controls in terms of body weight, fat and lean mass variation (Figure 5G, SF5), suggesting that energy expenditure resulting from increased physical activity was compensated by higher energetic supply. Cessation of CNO

administration progressively normalized both wheel running and food intake relative to controls, leading to significant gain in fat mass in the D1 Gq group (Figure 5G, SF5).

Chronic inhibition of D1-MSNs (D1 Gi) blunted wheel running, with no difference in food consumption compared to controls (Figure 5E, F). This resulted in significant weight gain and increase in fat mass as compared to the D1 Gq group (Figure 5G, SF5). Interestingly, lower voluntary physical activity was maintained despite cessation of CNO administration (Figure 5F) with no change in body weight or fat mass (Figure 5G, SF5).

Concomitant chronic manipulation of both MSN subpopulations bypasses the equilibrium between activity-related energy expenditure and energy intake

Altogether, our findings suggest that decreased energy expenditure due to lower voluntary wheel running, as observed under activation of D2-MSNs or inhibition of D1-MSNs, does not lead to compensatory decrease in food intake. Such an alteration of energy balance results in an obesity-like phenotype, which is in line with previous observation consecutive to decreased expression of the D2 receptor (Beeler et al., 2016; Friend et al., 2017) – which results in disinhibition of D2-MSNs. However, enhanced running-induced energy expenditure, as we found under D1-MSNs activation led to compensatory increase in food intake, thus maintaining energy balance, as reflected by the maintenance of weight and fat mass.

Considering the dichotomic effect of D1- and D2-MSN manipulations on energy intake and activity-related energy expenditure, we then tested whether the concomitant manipulation of both neuronal subpopulations would potentiate the aforementioned effects, eventually leading to bidirectional disruption of the balance between food intake and activity-induced energy expenditure. We took advantage of a unique mouse model expressing the flippase recombinase in D1-expressing neurons (Bonnavion et al., 2022) and crossed this mouse line with the D2-cre line, thereby allowing the concomitant manipulation of both NAc MSN subpopulations (Figure 6A). Simultaneous activation of D1-MSNs together with inhibition of D2-MSNs strongly increased wheel running. However, in this case, after an acute decrease the first day of CNO administration, food consumption remained equivalent to control animals (Figure 6B-C), leading to weight and fat loss (Figure 6D, SF6). In opposite, the concomitant inhibition of D1-MSNs together with activation of D2-MSNs resulted in significantly lower wheel running compared to controls, together with an initial increase in food consumption over the first 3 days, that returned to control levels thereafter (Figure 6B-C). Such a behavioral pattern resulted in weight gain and increased fat mass (Figure 6D, SF6). Cessation of CNO administration normalized voluntary physical activity in both groups (Figure 6C). Interestingly, this was accompanied by an increase of food intake (Figure 6B) and weight gain in animals in which D1- and D2-MSNs were previously activated and inhibited, respectively (Figure 6D,

SF6). Conversely, food intake (Figure 6B, SF6) and body weight (Figure 6D, SF6) were decreased in animals in which D1- and D2-MSNs were previously simultaneously inhibited and activated, respectively. Interestingly, the concomitant manipulations of D1- and D2-MSNs did not interfere with the ability of leptin and ghrelin to exert their respective anorexigenic and orexigenic effects (SF6), suggesting that the influence of MSN subpopulations on food intake is independent of such hormones.

To further assess to which extent the effect of chronic manipulation of MSNs on voluntary activity could overcome metabolic signals related to energy intake, animals were subjected to a gradual food deprivation in the presence of the running wheel. Under such conditions, all groups displayed a decrease in weight that was significantly enhanced under concomitant activation of D1-MSNs and inhibition of D2-MSNs. This effect was likely due to higher activity-related energy expenditure since these animals displayed higher voluntary wheel running despite food restriction (Figure 6E).

DISCUSSION

Beyond the well-documented role of NAc core MSNs in the modulation of incentive processes, the present study highlights an underestimated differential implication of D1- and D2-MSN subpopulations in the balance between food intake and physical activity-induced energy expenditure. As an illustration, the use of the above-mentioned double transgenic mice reveals that repeated (i) activation of D2-MSNs together with (ii) inhibition of D1-MSNs is sufficient to elicit an obesity-like phenotype as assessed by a decrease in energy expenditure. In opposite, repeated hyperactivity of D1-MSNs together with hypoactivity of D2-MSNs directs the energetic balance towards physical activity at the expense of energy intake, which are typical features of AN.

Even though dimensional approaches to EDs is just starting to emerge, increasing evidence supports alterations in common domains across EDs, especially those linked to reward-related positive valence system (Wildes and Marcus, 2015). In particular, reward valuation is elevated in individuals with obesity-related binge eating syndromes, but excessively diminished in patients with AN (Manwaring et al., 2011; Steinglass et al., 2012; Wierenga et al., 2015). Similarly, increased willingness to work for disorder-specific reward, i.e. exercise and food for AN and bulimia, respectively, are increased (Klein et al., 2010; Schebendach et al., 2013), suggesting that alterations in effort valuation are a main feature of EDs (Wildes and Marcus, 2015). Such reward-related symptoms correlate with opposite brain activity patterns, especially in cortico-striatal circuits (Kaye et al., 2013), hence reinforcing the hypothesis that overeating-related pathologies and AN correspond to the two ends of an ED spectrum. Our data suggest that opposite alterations in the activity of NAc MSN subcircuits could underlie a subset of

symptomatic dimensions of ED phenotypes, in particular the balance between calorie intake and activity-related energy expenditure.

Acute manipulations of the two subtypes of MSNs led to opposite consequences on food intake and voluntary physical activity in opposite manner highlighting the implication of these neuronal subpopulations in the regulation of energy balance. However, it is important to stress that, under chronic manipulations, the homeostatic system – likely comprising hypothalamic network - seems to be able to overcome alteration of MSNs' activity. Thus, under chronic activation of D1-MSNs, despite an acute decrease in food intake, enhanced energy expenditure through physical activity is accompanied by increased food intake, allowing maintenance of fat mass and body weight. It is only when both MSNs subpopulations are concomitantly manipulated, i.e. activation and inhibition of D1- and D2-MSNs, respectively, that such an homeostatic system does not fully compensate for energy expenditure, hence leading to weight loss. Nonetheless, animals still eat comparable amount of food than controls, suggesting that the energetic imbalance mainly results from exaggerated physical activity-mediated energy expenditure rather than reduced food consumption. Similarly, when D1-MSNs or D2-MSNs are respectively subjected to chronic inhibition and activation, weight/fat gain mostly originates from decreased physical activity since animals consume comparable amount of food than controls. Yet, avoidance and compulsion towards exercise are typical features of obesity-related disorders and AN, respectively, that have been proposed to be one main pathophysiological mechanism leading to, and even preceding, the development of EDs (Casper, 2006, 2018; Ekkekakis et al., 2016). Even though speculative, overall, our findings suggest that chronic dysfunction of NAc MSN network activity could participate to the etiology of EDs by altering, positively or negatively, the willingness to engage in, and/or the rewarding value of, physical activity.

Of importance is the observation that wheel-running, rather than reflecting non-specific locomotor responses, is a goal-directed behavior accounted for by the reinforcing value of exercise. Thus, as for other natural rewards such as food, rats/mice are willing to exert efforts, i.e. lever presses or nose pokes, to access a wheel (Collier and Hirsch, 1971; Iversen, 1993; Hurel et al., 2019). In accordance, our findings using chemogenetic inhibition demonstrate that D1-MSNs facilitate both wheel-running and willingness to exert effort to obtain a food reward, while D2-MSNs rather play an opposite role. These data further suggest that alterations in voluntary physical activity under MSNs manipulation reflect changes in reward/incentive processes and reveal the antagonistic role of the two NAc MSN subpopulations on this dimension. However, such an opposite effect of D1- and D2-MSNs on motivational processes has been recently challenged. Similarly to our findings, the chemogenetic inhibition of D2-MSNs of the NAc enhances performance in a motivational task (Carvalho Poyraz et al., 2016;

Gallo et al., 2018), while optogenetic manipulations of D2-MSNs of the NAc rather support a "pro-motivational" role, similarly to D1-MSNs (Natsubori et al., 2017; Soares-Cunha et al., 2016, 2018). However, recent data clarified this discrepancy, showing that optogenetic stimulation of D2-MSNs during reward-predicting cue enhances operant responding, while the very same manipulation during reward consumption has the opposite effect (Soares-Cunha et al., 2022). Such a dissociated role of D2-MSNs on distinct phases of the motivational dimension remains unclear and might involve reward prediction error mechanisms through dynamic feedback modulation of VTA dopamine neurons (Soares-Cunha et al., 2022). Nonetheless, our results support that chronic increase or decrease in D2-MSNs activity, as putatively found in some pathological conditions, will likely lead to enhanced and blunted motivational processes, respectively.

In addition to their antagonistic effect on the "ability to exert effort", our results reveal that D1-MSNs inhibit, whereas D2-MSNs of the NAc enhance food intake. While, to the best of our knowledge, such a role of D2-MSNs has not been reported before, the acute anorexigenic potency of D1-MSNs has been previously described for the NAc shell, through projections onto the lateral hypothalamus and the midbrain (Bond et al., 2020; O'Connor et al., 2015; Thoeni et al., 2020). Altogether, these observations suggest that, under physiological conditions, the recruitment of the NAc network in favor of D1-MSNs would bias behavior towards effort exertion – including food-seeking – at the expense of food consumption. In opposite, a predominant activity of D2-MSNs would blunt voluntary activity whilst promoting food intake. Such a pivotal role of the NAc MSN network is in accordance with the implication of the NAc as a "sensory sentinel", allowing rapid control over food consumption in response to motivational or sensory signals (Baldo and Kelley, 2007; Bond et al., 2020; Kelley et al., 2005; O'Connor et al., 2015). It remains to be determined whether these behavioral dimensions bidirectionally modulated by MSNs depend on distinct subpopulations in the NAc and/or their projecting areas. Nonetheless, the current work suggests that an imbalance in the MSN network of the NAc could be sufficient to alter homeostatic balance, eventually leading to EDs.

Acknowledgments: We thank the Bordeaux Imaging Center funded by ANR-10-INBS-04 for imaging, Motac Neuroscience for lending the rotarod apparatus, Céline Ducroix-Crépy and Jean-Christophe Helbling (INRAE UMR 1286) for genotyping and the staff from the animal facility of INRAE UMR 1286 for animal care.

Funding: This study was supported by INRAE and University of Bordeaux; Idex Bordeaux "chaire d'installation" (ANR-10-IDEX-03-02) (PT), NARSAD Young Investigator Grants from the Brain and Behavior Foundation (PT), ANR "SynLip" (ANR-16-CE16-0022) (PT), ANR "FrontoFat" (ANR-20-CE14-0020) (PT), ANR StriaPOM (ANR-21-CE14-0018) (PT), Institut de Recherche en Santé publique (IReSP) Aviesan APP-addiction 2019 (PT), Labex "BRAIN" (PT and RW), Region Nouvelle Aquitaine 2014-1R30301-00003023 (PT); Fondation pour la Recherche Médicale (FRM "Environnement et Santé") (GF and PT), ANR "HA-CTion" (ANR-19-HBPR-0002) (GF and PT); PRESTIGE-2017-2-0031 (AC), "Fondation pour la Recherche Médicale" SPF201809007095 (AC); Canadian Institute for Health Research (201309OG-312343-PT; 201803PJT-399980-PT) (BG); FD and RW are recipients of PhD fellowships from the French Ministry of Research. AP is a recipient of a PhD fellowship from the "Ecole Universitaire de Recherche" (EUR Neuro, Bordeaux Neurocampus); AKE is Research Director of FRS-FNRS and WELBIO investigator. AKE was supported by grants from from FRS-FNRS (#23587797, #33659288, #33659296), Fondation Simone et Pierre Clerdent (Prize 2018) and Fondation ULB.

Authors contributions: RW, GF, FD, FG and PT designed research, RW, AP, GRF, AC, RO, AO, VDP and FD performed research, RW, FD, FG and PT supervised research, RW, AP, GRF, AC, FD, FG and PT analyzed data, AKE, BG and FC provided expertise, reagents and material, RW, FC, GF, FD, FG and PT wrote the manuscript. All authors edited and approved the manuscript.

Declaration of interests: The authors declare no competing interests.

FIGURE LEGENDS

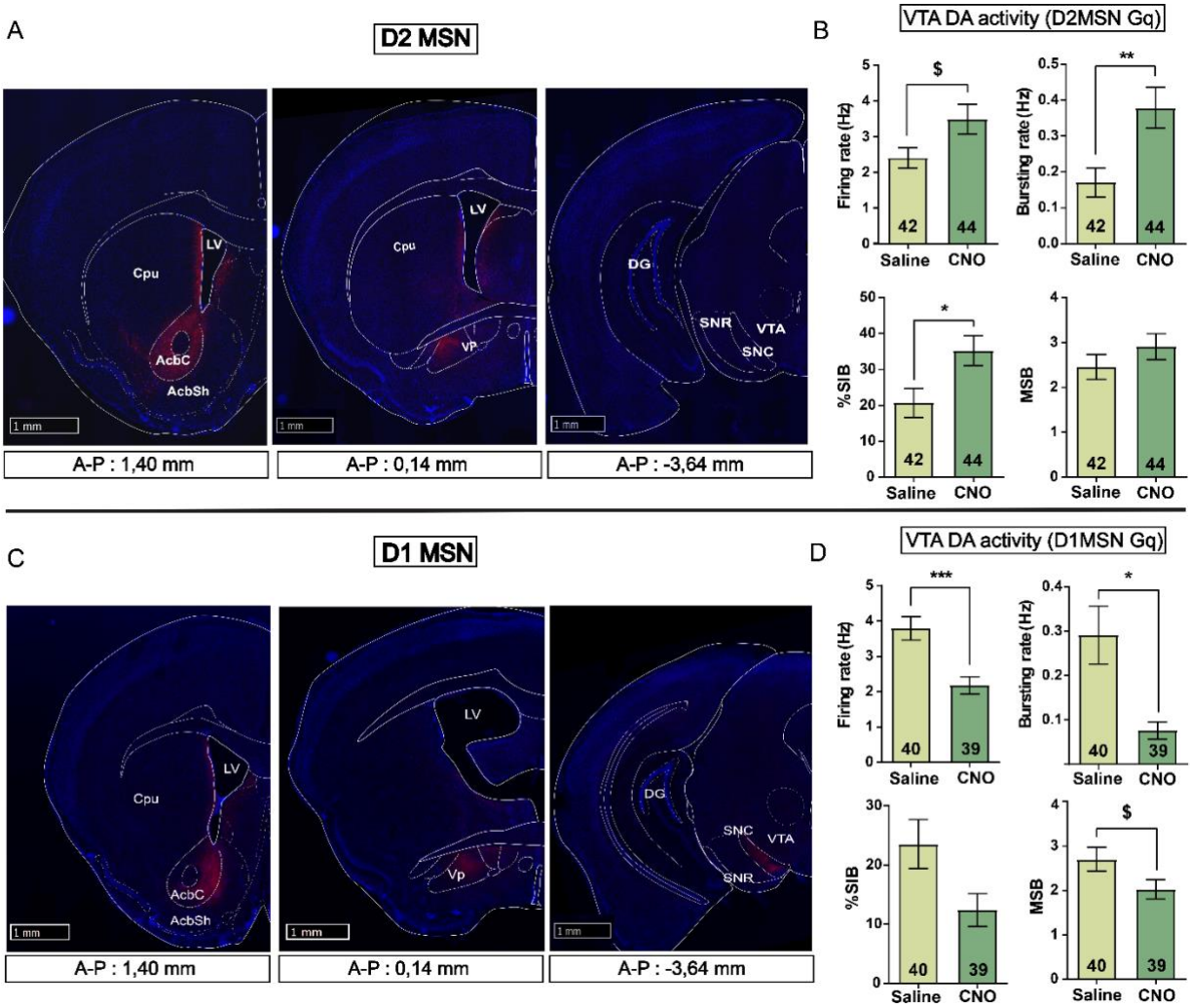

Figure 1 : NAc D2-MSNs and D1-MSNs inhibit and potentiate the activity of VTA dopaminergic neurons, respectively.

(A) Representative coronal sections for mCherry expression after injection of a cre-dependent DREADD-mCherry-carrying viral vector in D2-cre mice. Transduction is mostly restricted to the NAc core (left), leading to detection of projections in the ventral pallidum (VP, middle) but not in the midbrain (right). (B) In vivo recording of DA neurons of the VTA in D2-cre mice expressing the activating DREADD HM3Dq showing that, compared to saline, CNO (2 mg/kg) injection leads to a trend of an increase in firing rate (top left) and significant increase in bursting rate (top right) and % spike in burst (SIB, bottom left) while the mean spike in burst is spared (MSB, bottom right). Numbers in bars indicate the number of neurons recorded (D2-Gq mice n=6). (C) Representative coronal sections for mCherry expression after injection of a cre-dependent DREADD-mCherry-carrying viral vector in D1-cre mice. Transduction is mostly restricted to the NAc core (left), leading to detection of projections in the ventral pallidum (VP,

middle) as well as in the midbrain (right). (D) In vivo recording of DA neurons of the VTA in D1-cre mice expressing the activating DREADD HM3Dq showing that, compared to saline, CNO (2 mg/kg) injection leads to a significant decrease in firing and bursting rates (top) but spared %SIB and MSB (bottom). Numbers in bars indicate the number of neurons recorded (D1-Gq mice n=4). $: 0.05<p<0.1 ; * : p<0.05 ; ** : p<0.01 ; *** : p<0.001 ; Error bars = s.e.m. See Table 2 for statistical analyses.

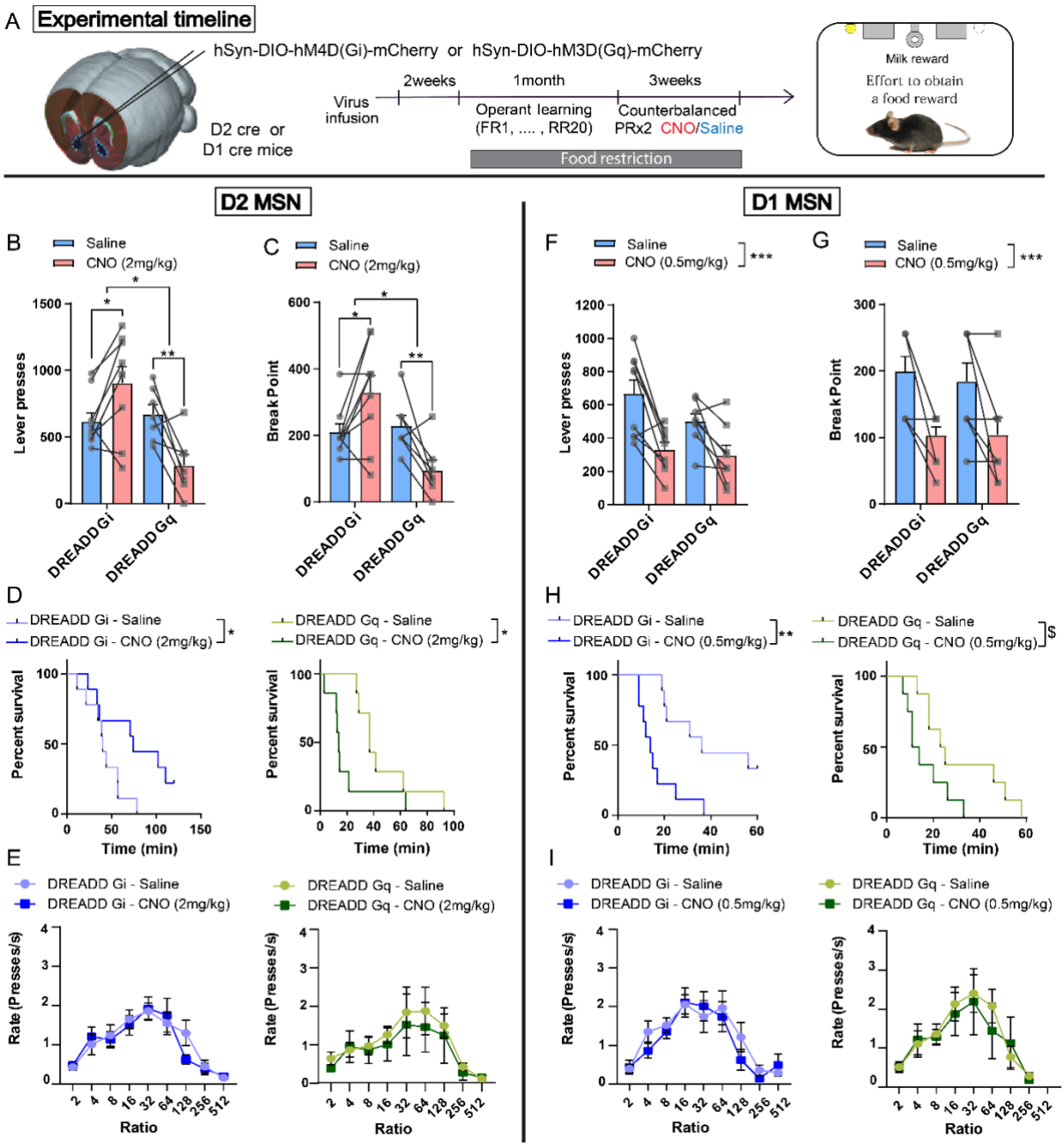

Figure 2: Effect of chemogenetic manipulations of D2- and D1-MSNs of the NAc on the motivational dimension of feeding behavior.

(A) Experimental timeline. (B-E) Chemogenetic-mediated D2-MSNs activation (DREADD Gq) and inhibition (DREADD Gi) under administration of CNO at 2 mg/kg respectively decrease and increase the number of reinforced lever presses (B), breakpoint (C) and the percentage of mice that keep on responding as a function of time (D) in the PR schedule. Changes in operant responding is not related to alterations in ratio requirement plotted as the rate of lever presses as a function of PR ratios (E). (F-I) Chemogenetic-mediated D1-MSNs activation

(DREADD Gq) and inhibition (DREADD Gi) with CNO at 0.5 mg/kg decrease the number of reinforced lever presses (F), break point (G) and the percentage of mice that keep on responding as a function of time (H) in the PR schedule. Ratio requirement is spared (I). Data are averages of 2 PR sessions under CNO or saline administrations in a within-subject, counterbalanced manner. D2-cre: DREADD Gi n=9, DREADD Gq n=7; D1-cre: DREADD Gi n=9, DREADD Gq n=8. * : $p<0.05$; ** : $p<0.01$; *** : $p<0.001$; Error bars = s.e.m. See Table 2 for statistical analyses.

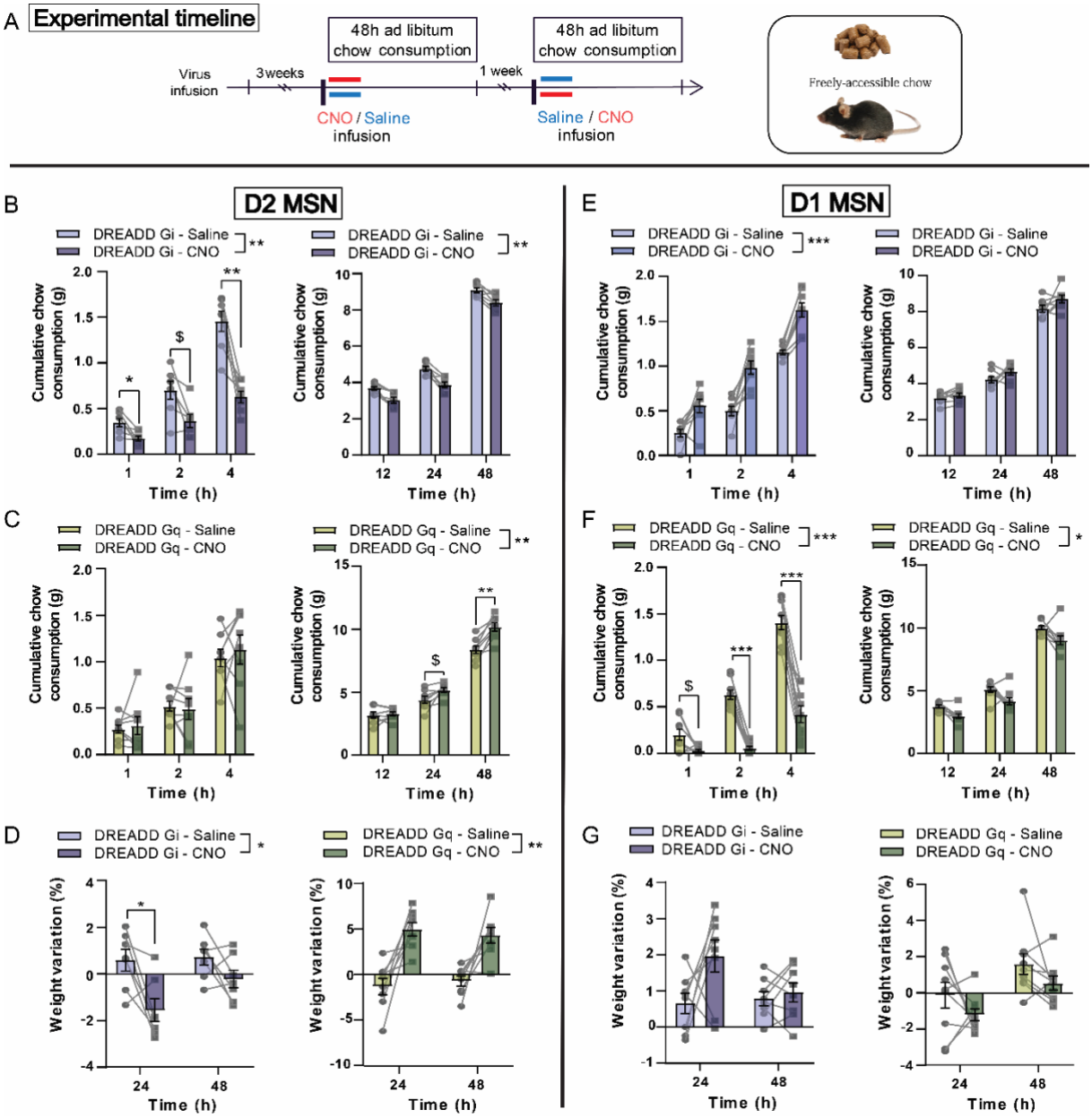

Figure 3: Effect of chemogenetic manipulations of D2- and D1-MSNs of the NAc on *ad libitum* food consumption.

(A) Experimental timeline. (B-D) Chemogenetic-mediated inhibition of D2-MSNs (DREADD Gi) decreases food consumption as shown by cumulative food intake (B), while their activation (DREADD Gq) increases food consumption with a delayed effect (24-48h) (C). These effects on food intake lead to significant changes in body weight at 24-48h (D). (E-G) Chemogenetic-mediated inhibition (E) and activation (F) of D1-MSNs increases and decreases food intake, respectively, with no significant change on weight variation at 24-48h (G). (CNO: 2mg/kg); D2-cre: DREADD Gi n=7, DREADD Gq n=8; D1-cre: DREADD Gi n=8, DREADD Gq n=9. * : p<0.05 ; ** : p<0.01 ; *** : p<0.001 ; Error bars = s.e.m. See Table 2 for statistical analyses.

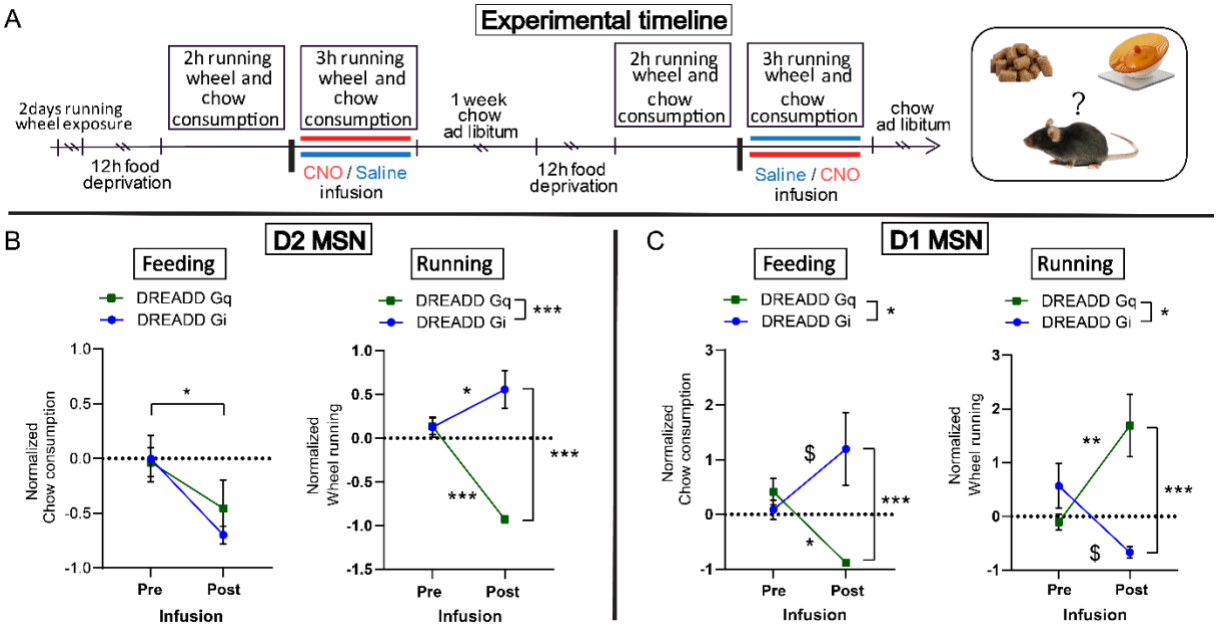

Figure 4: Effect of chemogenetic manipulations of D2- and D1-MSNs of the NAc in a wheel-running/free-feeding choice procedure.

(A) Experimental timeline. (B-C) Normalized chow consumption and wheel running comparing 1-hour pre-CNO and 1-hour post-CNO injection. Both D2-MSNs activation and inhibition lead to decreased food intake (B, left). D2-MSNs activation strongly decreases, while their inhibition diminishes, wheel running (B, right). D1-MSNs inhibition increases food intake and decreases wheel-running, while their activation decreases and increases food intake and wheel-running respectively (B). (CNO : 2mg/kg). D2-cre: DREADD Gi n=7, DREADD Gq n=7 ; D1-cre: DREADD Gi n=8, DREADD Gq n=8. * : $p<0.05$; ** : $p<0.01$; *** : $p<0.001$; Error bars = s.e.m. See Table 2 for statistical analyses.

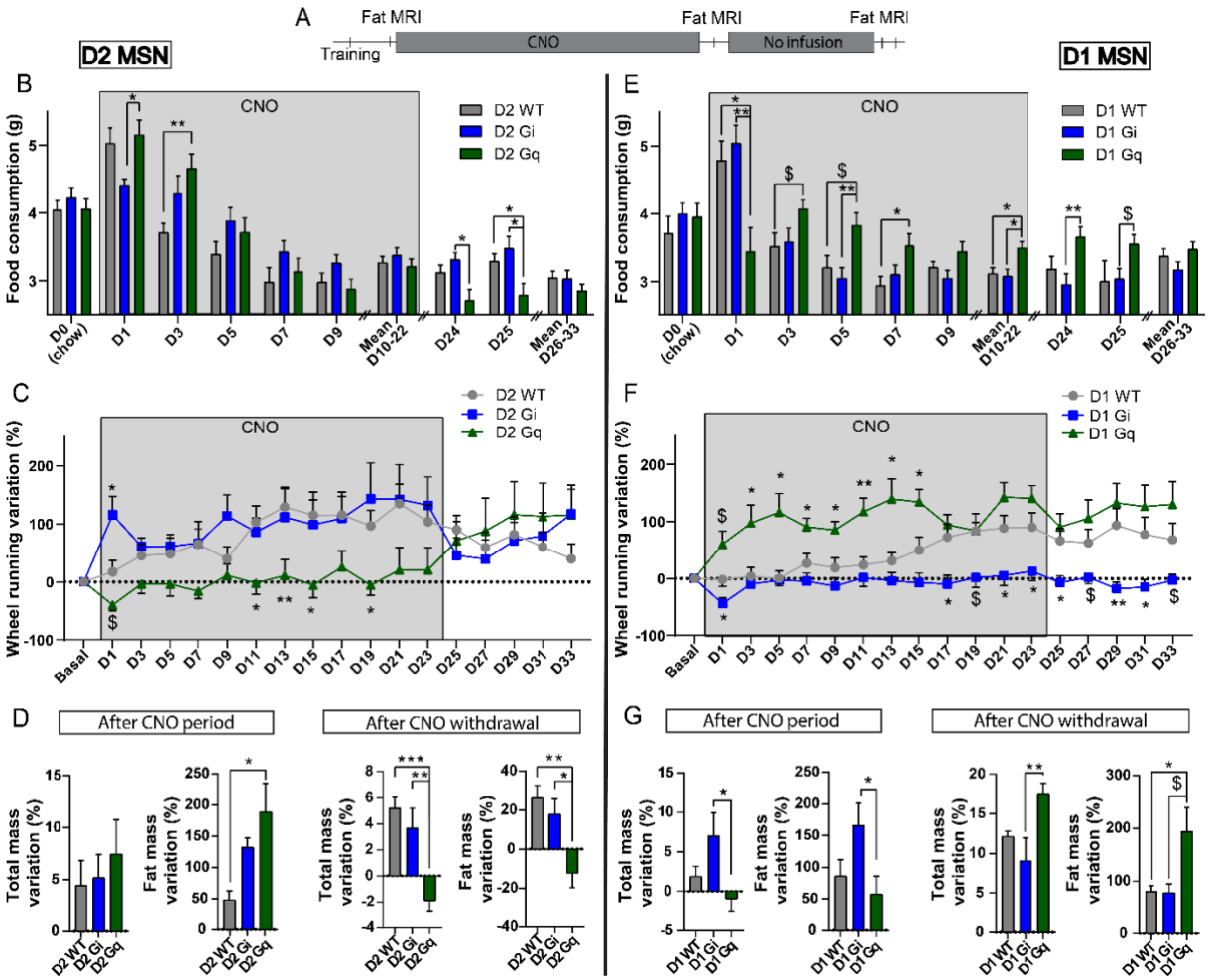

Figure 5: Effect of chronic chemogenetic manipulations of D2-MSNs and D1-MSNs of the NAc in a wheel-running/free-feeding choice procedure.

(A) Experimental design. (B-D) Food consumption over time (B), variation in wheel running (C) and variation in total and fat mass (D) were measured under chronic D2-MSNs inhibition (D2 Gi) and activation (D2Gq) compared to WT controls, as well as after CNO cessation. (E-G) The same design was followed for chronic D1-MSNs manipulations. (CNO: 2mg/kg); D2- WT n=9; D2-Gi n=8; D2-Gq n=9; D1-WT n=12; D1-Gi n=11; D1-Gq n=12. $: 0.05<p<0.1; *: p<0.05; **: p<0.01; Error bars = s.e.m. See Table 2 for statistical analyses.

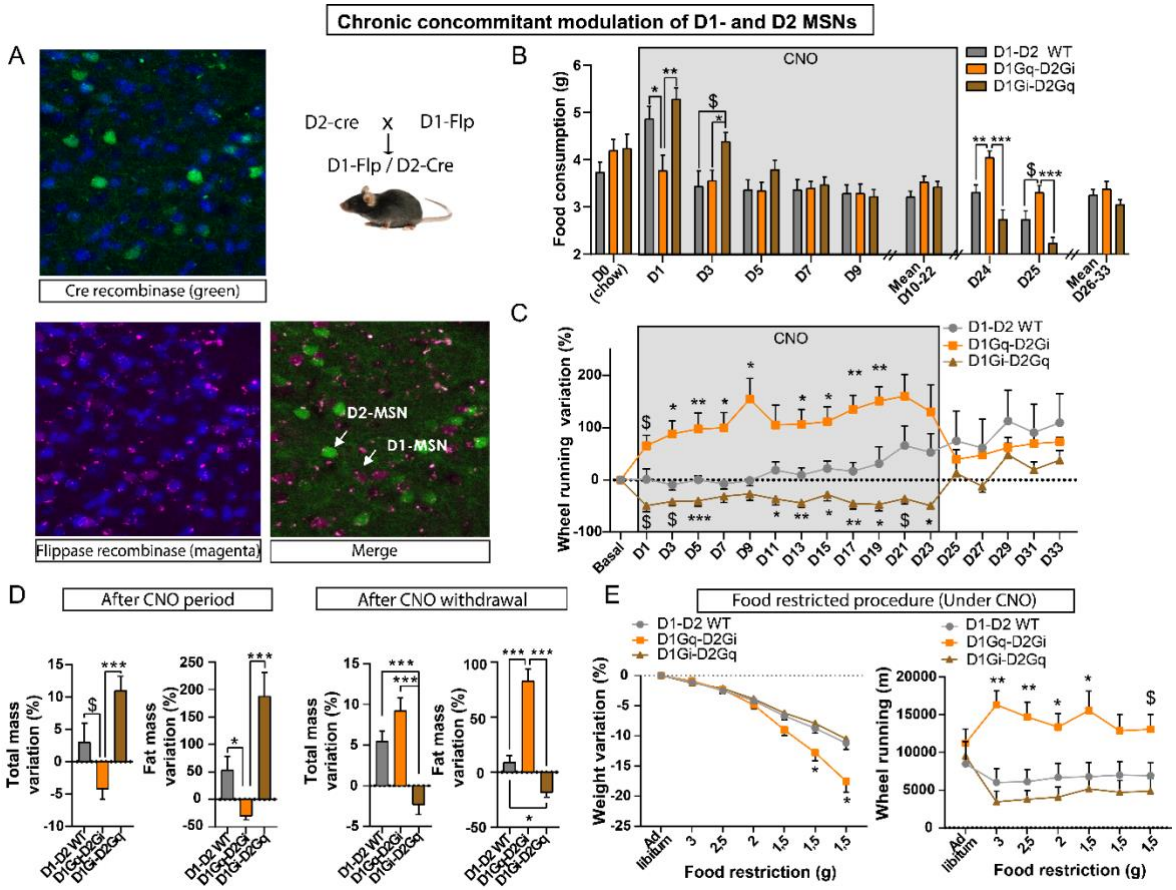

Figure 6: Effect of chronic and simultaneous chemogenetic manipulations of D2-MSNs and D1-MSNs of the NAc in a wheel-running/free-feeding choice procedure.

(A) Pattern of expression of cre and flp in double transgenic D1-FlpxD2-cre mice showing a virtually complete exclusion of expressions. (B-D) Food consumption over time (B), variation in wheel running (C) and variation in total and fat mass (D) were measured under chronic manipulations of both MSN populations (D1Gq-D2Gi: concomitant activation of D1-MSNs and inhibition of D2-MSNs; D1Gi-D2Gq: concomitant inhibition of D1-MSNs and activation of D2-MSNs) compared to WT controls, as well as after CNO cessation. (E) Weight variation (left) and wheel running (right) were recorded during a gradual food restriction procedure under chronic CNO. (CNO: 2mg/kg); D1-D2 WT n=11 ; D1Gi-D2Gq n=11, D1Gq-D2Gi n=8. $: 0.05<p<0.1 * : p<0.05 ; ** : p<0.01; *** : p<0.001 Error bars = s.e.m. See Star methods for statistical analyses.

Table 1: Key resources

REAGENT or RESOURCE	SOURCE	IDENTIFIER
Antibodies		
Primary antibody anti-DSred (rabbit)	Takara Bio	632496
Primary antibody anti-Choline acetyl transferase (goat)	Merck Millipore	AB144P
Primary antibody anti-cre (rabbit)	Produced by the Laboratory of C. Kellendonk	N/A
Secondary antibody anti-rabbit alexa 568 (donkey)	ThermoFisher	A-10042
Secondary antibody anti-rabbit alexa 488 (donkey)	ThermoFisher	A-21206
Secondary antibody anti-goat alexa 568 (donkey)	ThermoFisher	A-11057
Secondary antibody anti-goat alexa 488 (donkey)	ThermoFisher	A-11055
Bacterial and Virus Strains		
AAV8-hSyn-DIO-hM4D(Gi)-mCherry	Addgene	44362-AAV8
AAV8-hSyn-DIO-hM4D(Gi)-mCherry	Zurich vector Core	V84
AAV8-hSyn-DIO-hM3D(Gq)-mCherry	Addgene	44361-AAV8
AAV8-hSyn-DIO-hM3D(Gq)-mCherry	Zurich vector Core	V89
AAV8-hSyn1-dFRT-hM4D(Gi)-mCherry(rev)-dFRT-WPRE-hGHp(A)	Zurich vector Core	V189
AAV8-hSyn1-dFRT-hM3D(Gq)-mCherry(rev)-dFRT-WPRE-hGHp(A	Zurich vector Core	V190
Chemicals, Peptides, and Recombinant Proteins		
Clozapine-N-Oxide (CNO)	ENZO	BML-NS105
Recombinant Mouse Leptin Protein, CF	Bio-Techne	498-OB-05M
Ghrelin	Bachem	H-4862.1000
Critical Commercial Assays		
ACCU-CHEK Performa	Roche	N/A
Experimental Models: Organisms/Strains		
Mouse: C57BL/6J	Janvier Labs	N/A
Mouse: Tg(Drd1-cre)FK150Gsat/Mmucd	GENSAT	RRID: MMRRC_029178-UCD
Mouse: Tg(Drd2-cre)ER44Gsat/Mmucd	GENSAT	RRID: MMRRC_017263-UCD
Mouse D1Flp (D1 expressing flippase and YFP)	Produced by the Laboratory of B. Giros	N/A

Table 2: Summary of statistical analyses

Data	Statistical test	n	Outcome measure	P value
Figure 1				
Figure 1B	Mann Whitney test	D2cre mice (n=6), neurons Saline:42 / CNO:44	Firing rate (Hz)	U=712, P= 0.0612
Figure 1B	Mann Whitney test	D2cre mice (n=6), neurons Saline:42 / CNO:44	Bursting rate (Hz)	U=579.5, P=0.0026
Figure 1B	Mann Whitney test	D2cre mice (n=6), neurons Saline:42 / CNO:44	%SIB	U=627, P= 0.0097
Figure 1B	Mann Whitney test	D2cre mice (n=6), neurons Saline:42 / CNO:44	MSB	U=791, P= 0.2369
Figure 1D	Unpaired T-test	D1cre mice (n=4), neurons Saline:40 / CNO:39	Firing rate (Hz)	t(77)=3.888, p=0.0002
Figure 1D	Mann Whitney test	D1cre mice (n=4), neurons Saline:40 / CNO:39	Bursting rate (Hz)	U=530.5, P=0.0133
Figure 1D	Mann Whitney test	D1cre mice (n=4), neurons Saline:40 / CNO:39	%SIB	U=634.5, P= 0.1534
Figure 1D	Unpaired T-test	D1cre mice (n=4), neurons Saline:40 / CNO:39	MSB	t(77)=1.953, p=0.0545
Figure 2				
Figure 2B	Two-way RM ANOVA	D2 cre mice: Dreadd Gi = 9 Dreadd Gq= 7	Lever presses	Virus effect F(1, 14)=6.604 P=0.0222 CNO effect F(1, 14)=0.3902 P=0.5423 Interaction F(1, 14)=19.29 P=0.0006 Bonferroni's multiple comparisons test: DREADD Gi : Sal vs CNO p=0.0258 DREADD Gq : Sal vs CNO p=0.0096
Figure 2B	Two-way RM ANOVA	D2 cre mice: Dreadd Gi = 9 Dreadd Gq= 7	Break point	Virus effect F(1, 14)=6.773 P=0.0209 CNO effect F(1, 14)=0.04977 P=0.8267 Interaction F(1, 14)=14.92 P=0.0017 Bonferroni's multiple comparisons test: DREADD Gi : Sal vs CNO p=0.0310 DREADD Gq : Sal vs CNO p=0.0327
Figure 2D	Log-rank (Mantel-Cox) test	D2 cre mice: Dreadd Gi = 9	Survival Curve	$\chi 2$=4.511 ; P Value=0.0337
Figure 2D	Gehan-Breslow-Wilcoxon test	D2 cre mice: Dreadd Gq= 7	Survival Curve	$\chi 2$=6.338 ; P Value=0.0118
Figure 2E	Mixed-effects model (Geisser-Greenhouse's epsilon correction)	D2 cre mice: Dreadd Gi = 9	Rate (presses/s)	Ratio effect F(3.138, 25.10)=20.67 P<0.0001 (ε correction : 0.3922) CNO effect F(1.000, 8.000)=0.1515 P=0.7073 (ε correction : 1.000) Interaction F(3.379, 27.03)=1.024 P=0.4040 (ε correction : 0.4224)
Figure 2E	Mixed-effects model (Geisser-Greenhouse's epsilon correction)	D2 cre mice: Dreadd Gq= 7	Rate (presses/s)	Ratio effect F(1.245, 7.469)=4.953 P=0.0539 (ε correction : 0.1556) CNO effect F(1.000, 6.000)=2.183 P=0.1900 (ε correction : 1.000) Interaction F(2.468, 12.34)=0.7316 P=0.5278 (ε correction : 0.3085)

Figure 2F	Two-way RM ANOVA	D1 cre mice: Dreadd Gi = 9 Dreadd Gq=8	Lever presses	Virus effect F(1, 15)=1.992 P=0.1785 CNO effect F(1, 15)=28.22 P<0.0001 Interaction F(1, 15)=1.658 P=0.2174
Figure 2G	Two-way RM ANOVA	D1 cre mice: Dreadd Gi = 9 Dreadd Gq=8	Break point	Virus effect F(1, 15)=0.06963 P=0.7955 CNO effect F(1, 15)=25.29 P=0.0001 Interaction F(1, 15)=0.2090 P=0.6541
Figure 2H	Log-rank (Mantel-Cox) test	D1 cre mice: Dreadd Gi = 9	Survival Curve	$\chi 2$=8.910 ; P Value=0.0028
Figure 2H	Log-rank (Mantel-Cox) test	D1 cre mice: Dreadd Gq= 8	Survival Curve	$\chi 2$=3.652 ; P Value=0.0560
Figure 2I	Mixed-effects model (Geisser-Greenhouse's epsilon correction)	D1 cre mice: Dreadd Gi = 9	Rate (presses/s)	Ratio effect F(2.171, 17.37)=17.20 P<0.0001 (ε correction : 0.2713) CNO effect F(1, 8)=1.422 P=0.2673 (ε correction : 1.000) Interaction F(2.167, 14.90)=1.135 P=0.3517 (ε correction : 0.2709)
Figure 2I	Mixed-effects model (Geisser-Greenhouse's epsilon correction)	D1 cre mice: Dreadd Gq=8	Rate (presses/s)	Ratio effect F(1.361, 9.525)=9.687 P<0.0001 (ε correction : 0.1944) CNO effect F(1, 7)=0.3425 P=0.5768 (ε correction : 1.000) Interaction F(2.055, 13.80)=1.131 P=0.3605 (ε correction : 0.2936)
Figure 3				
Figure 3B	Mixed-effects model (Geisser-Greenhouse's epsilon correction)	D2 cre mice Dreadd Gi = 7	Cumulative Chow consumption (1h - 4h)	Time effect F(1.537, 9.224)=135.9 P<0.0001 (ε correction : 0.7687) CNO effect F(1.000, 6.000)=23.20 P=0.0029 (ε correction : 1.000) Interaction F(1.826, 10.96)= 23.79 P=0.0001 (ε correction : 0.9130) Bonferroni's multiple comparisons test: DREADD Gi Sal vs CNO: 1h p=0.0488; 2h p<0.0527; 4h p=0.0042
Figure 3B	Mixed-effects model (Geisser-Greenhouse's epsilon correction)	D2 cre mice Dreadd Gi = 7	Cumulative Chow consumption (12h - 48h)	Time effect F(1.973, 12.84)=3332 P<0.0001 (ε correction : 0.9863) CNO effect F(1.000, 6.000)=25.13 P=0.0024 (ε correction : 1.000) Interaction F(1.158, 6.9472)=1.009 P=0.3630 (ε correction : 0.3630)
Figure 3C	Mixed-effects model (Geisser-Greenhouse's epsilon correction)	D2 cre mice Dreadd Gq = 8	Cumulative Chow consumption (1h - 4h)	Time effect F(1.083, 7.584)=154.1 P<0.0001 (ε correction : 0.5417) CNO effect F(1.000, 7.000)=0.09415 P=0.7679 (ε correction : 1.000) Interaction F(1.100, 7.898)=0.4557 P=0.5376 (ε correction : 0.5499)

Figure 3C	Mixed-effects model (Geisser-Greenhouse's epsilon correction)	D2 cre mice Dreadd Gq = 8	Cumulative Chow consumption (12h - 48h)	Time effect F(1.352, 9.461)=1206 P<0.0001 (ε correction : 0.6758) CNO effect F(1.000, 7.000)=15.05 P=0.0061 (ε correction : 1.000) Interaction F(1.180, 8.260)=25.34 P=0.0007 (ε correction : 0.5900) Bonferroni's multiple comparisons test: DREADD Gq Sal vs CNO: 12h p>0.9999; 24h p<0.0011; 48h p<0.0001
Figure 3D	Mixed-effects model (Geisser-Greenhouse's epsilon correction)	D2 cre mice Dreadd Gi = 7	Weight variation	Time effect F(1.000, 6.000)=19.95 P=0.0043 (ε correction : 1.000) CNO effect F(1.000, 6.000)=7.204 P=0.0363 (ε correction : 1.000) Interaction F(1.000, 6.000)=13.50 P=0.0104 (ε correction : 1.000) Šídák's multiple comparisons test : DREADD Gq Sal vs CNO: 24h p=0.0500; 48h p=0.2485
Figure 3D	Mixed-effects model (Geisser-Greenhouse's epsilon correction)	D2 cre mice Dreadd Gq = 8	Weight variation	Time effect F(1.000, 7.000)=0.008117 P=0.9307 (ε correction : 1.000) CNO effect F(1.000, 7.000)=26.40 P=0.0013 (ε correction : 1.000) Interaction F (1.000, 7.000) = 1.854 P=0.2155 (ε correction : 1.000)
Figure 3E	Mixed-effects model (Geisser-Greenhouse's epsilon correction)	D1 cre mice Dreadd Gi = 8 1 D1Gi were excluded with Grubbs' method (Alpha = 0.01)	Cumulative Chow consumption (1h - 4h)	Time effect F(1.271, 8.896)=242.4 P<0.0001 (ε correction : 0.6355) CNO effect F(1.000, 7.000)=35.33 P=0.0005 (ε correction : 1.000) Interaction F(1.555, 10.88)=3.055 P=0.0975 (ε correction : 0.7773)
Figure 3E	Mixed-effects model (Geisser-Greenhouse's epsilon correction)	D1 cre mice Dreadd Gi = 8 1 D1Gi were excluded with Grubbs' method (Alpha = 0.01)	Cumulative Chow consumption (12h - 48h)	Time effect F(1.263, 8.839)=1072 P<0.0001 (ε correction : 0.6314) CNO effect F(1.000, 7.000)=3.908 P=0.0886 (ε correction : 1.000) Interaction F(1.839, 12.87)=1.434 P=0.2723 (ε correction : 0.9194)
Figure 3F	Mixed-effects model (Geisser-Greenhouse's epsilon correction)	D1 cre mice Dreadd Gq = 9	Cumulative Chow consumption (1h - 4h)	Time effect F(1.150, 9.198)=156.9 P<0.0001 (ε correction : 0.5749) CNO effect F(1.000, 8.000)=108.8 P<0.0001 (ε correction : 1.000) Interaction F(1.136, 9.086)=40.59 P<0.0001 (ε correction : 0.5679) Bonferroni's multiple comparisons test: DREADD Gq Sal vs CNO: 1h p=0.0840; 2h p<0.0001; 4h p<0.0001
Figure 3F	Mixed-effects model (Geisser-Greenhouse's epsilon correction)	D1 cre mice Dreadd Gq = 9 1 outlier value removed with Grubbs' method (Alpha = 0.01)	Cumulative Chow consumption (12h - 48h)	Time effect F(1.948, 18.58)=1293 P<0.0001 (ε correction : 0.9738) CNO effect F(1.000, 8.000)=14.62 P=0.0051 (ε correction : 1.000) Interaction F(1.342, 9.392)=0.2907 P=0.3203 (ε correction : 0.6708)

Figure 3G	Mixed-effects model (Geisser-Greenhouse's epsilon correction)	D1 cre mice Dreadd Gi = 8 1 D1Gi were excluded with Grubbs' method (Alpha = 0.01)	Weight variation	Time effect F(1.000, 7.000)=3.292 P=0.1125 (ε correction : 1.000) CNO effect F(1.000, 7.000)=3.695 P=0.0960 (ε correction : 1.000) Interaction F(1.000, 7.000)=5.499 P=0.0515 (ε correction : 1.000)
Figure 3G	Mixed-effects model (Geisser-Greenhouse's epsilon correction)	D1 cre mice Dreadd Gq = 9	Weight variation	Time effect F(1.000, 8.000)= 26.45 P=0.0009 (ε correction : 1.000) CNO effect F(1.000, 8.000)=2.831 P=0.1310 (ε correction : 1.000) Interaction F(1.000, 8.000)=0.001205 P=0.9732 (ε correction : 1.000)
Figure 4				
Figure 4B	Two-way RM ANOVA	D2Gi = 7 D2Gq = 7 1 D2Gq was excluded with Grubbs' method (Alpha = 0.01)	Chow consumption (ratio CNO/SAL)	Infusion effect F(1, 12)=8.570 P=0.0127 Virus effect F(1, 12)=0.3412 P=0.5700 Interaction F(1, 12)=0.5111 P=0.4823
Figure 4B	Two-way RM ANOVA	D2Gi = 7 D2Gq = 7 1 D2Gq was excluded with Grubbs' method (Alpha = 0.01)	Wheel running activity (ratio CNO/SAL)	Infusion effect F(1, 12)=8.410 P=0.0113 Virus effect F(1, 12)=23.88 P=0.0004 Interaction F(1, 12)=46.90 P<0.0001 Bonferroni's multiple comparisons test: D2Gi vs D2Gq: Pre infusion p>0.9999 ; Post infusion p<0.0001 Pre infusion vs Post infusion : D2Gi p=0.0326 D2Gq p<0.0001
Figure 4C	Two-way RM ANOVA	D1Gi = 8 D1Gq = 8 1 D1Gi and 1 D2Gq were excluded with Grubbs' method (Alpha = 0.01)	Chow consumption (ratio CNO/SAL)	Infusion effect F(1, 14)=0.06936 P=0.7961 Virus effect F(1, 14)=5.686 P=0.0318 Interaction F(1, 14)=10.97 P=0.0058 Bonferroni's multiple comparisons test: D1Gi vs D1Gq: Pre infusion p>0.9999 ; Post infusion p=0.0008 Pre infusion vs Post infusion : D1Gi p=0.0980 D1Gq p=0.0483
Figure 4C	Two-way RM ANOVA	D1Gi = 8 D1Gq = 8 1 D1Gi and 1 D2Gq were excluded with Grubbs' method (Alpha = 0.01)	Wheel running activity (ratio CNO/SAL)	Infusion effect F(1, 14)=0.6277 P=0.4414 Virus effect F(1, 14)=4.852 P=0.0449 Interaction F(1, 14)=18.60 P=0.0007 Bonferroni's multiple comparisons test: D1Gi vs D1Gq: Pre infusion p=0.4164 ; Post infusion p=0.0002 Pre infusion vs Post infusion : D1Gi p=0.0520 D1Gq p=0.0057
Figure 5				
Figure 5B	Mixed-effects model (Geisser-Greenhouse's epsilon correction)	D2 WT = 9 D2 GI = 8 D2 Gq = 9	High fat consumption D1-9 ; D24-25	Time effect F(3.466, 79.71)=70.40 P<0.0001 (ε correction : 0.3851) Virus effect F(2, 23)=0.6509 P=0.5309 Interaction F(18.207)=4.489 P<0.0001 Bonferroni's multiple comparisons test: D2Gq vs D2WT: Day3 p=0.0091; Day25 p=0.0330

				D2Gq vs D2Gi: Day1 p=0.0256; Day24 p=0.0197; Day25 p=0.0312
Figure 5B	One way ANOVA	D2 WT = 9 D2 GI = 8 D2 Gq = 9	High fat consumption mean D10-D22	F(2, 23)=0.6708 P=0.5210
Figure 5B	One way ANOVA	D2 WT = 9 D2 GI = 8 D2 Gq = 9	High fat consumption mean D26-D33	F(2, 23)=1.567 P=0.2302
Figure 5C	Mixed-effects model (Geisser-Greenhouse's epsilon correction)	D2 WT = 7 D2 GI = 7 D2 Gq = 8 (2 WT, 1 D1-Gi and 1 D1-Gq animals were exposed to a running wheel without recording) 5 outlier values removed with Grubbs' method (Alpha = 0.01)	Running wheel variation D1-9 ; D24-25	Time effect F(3.868, 72.36)=4.052 P=0.0055 (ε correction : 0.2276) Virus effect F(2, 19)=1.659 P=0.2167 Interaction F(34, 318)=3.536 P<0.0001 Bonferroni's multiple comparisons test: D2Gi vs D2WT: Day1 p=0.0272 D2Gq vs D2WT: Day11 p=0.0305; Day13 p=0.0038; Day15 p=0.0208 ; Day19 p=0.0328 ; Day21 p=0.0145 ; Day23 p=0.0228
Figure 5D	One way ANOVA	D2 WT = 9 D2 GI = 8 D2 Gq = 9	Weight variation following CNO period	F(2, 23)=0.3597 P=0.7017
Figure 5D	One way ANOVA	D2 WT = 9 D2 GI = 8 D2 Gq = 9 1 outlier value removed with Grubbs' method (Alpha = 0.01)	Fat mass variation following CNO period	F(2, 22)=5.397 P=0.0124 Bonferroni's multiple comparisons test: D2WT vs D2Gq p=0.0104
Figure 5D	One way ANOVA	D2 WT = 9 D2 GI = 8 D2 Gq = 9	Weight variation following CNO withdrawal	F(2, 23)=12.67 P=0.0002 Bonferroni's multiple comparisons test: D2WT vs D2Gq p=0.0002 D2Gi vs D2Gq p=0.0040
Figure 5D	One way ANOVA	D2 WT = 9 D2 GI = 8 D2 Gq = 9	Fat mass variation following CNO withdrawal	F(2, 23)=8.537 P=0.0017 Bonferroni's multiple comparisons test: D2WT vs D2Gq p=0.0020 D2Gi vs D2Gq p=0.0184
Figure 5E	Mixed-effects model (Geisser-Greenhouse's epsilon correction)	D1 WT = 12 D1 GI = 11 D1 Gq = 12 2 outlier values removed with Grubbs' method (Alpha = 0.01)	High fat consumption D1-9 ; D24-25	Time effect F(3.418, 108.4)=34.19 P<0.0001 (ε correction : 0.4883) Virus effect F(2, 32)=1.470 P=0.2451 Interaction F(14.222)=6.702 P<0.0001 Bonferroni's multiple comparisons test: D1Gq vs D1WT: Day1 p=0.0183; Day3 p=0.0771; Day5 p=0.0612; Day7 p=0.0411 D1Gq vs D1Gi: Day1 p=0.0022; Day5 p=0.0096; Day24 p=0.0082; Day25 p=0.0558
Figure 5E	One way ANOVA	D1 WT = 12 D1 GI = 11 D1 Gq = 12	High fat consumption mean D10-D22	F(2, 32)=6.579 P=0.0040 Bonferroni's multiple comparisons test: D1Gq vs D1WT: p=0.0152 D1Gq vs D1Gi: p=0.0084
Figure 5E	One way ANOVA	D1 WT = 12 D1 GI = 11 D1 Gq = 12	High fat consumption mean D26-D33	F(2, 32)=2.153 P=0.1327

Figure 5F	Mixed-effects model (Geisser-Greenhouse's epsilon correction)	D1 WT = 9 D1 GI = 11 D1 Gq = 11 (3 WT and 1 D1-Gq animals were exposed to a running wheel without recording) 1 outlier value removed with Grubbs' method (Alpha = 0.01)	Running wheel variation D1-9 ; D24-25	Time effect F(4.651, 128.9)=10.12 P<0.0001 (ε correction : 0.2736) Virus effect F(2, 28)=11.07 P=0.0003 Interaction F(34.471)=3.334 P<0.0001 Bonferroni's multiple comparisons test: D1Gq vs D1WT: Day1 p=0.0531; Day3 p=0.0223; Day5 p=0.0129; Day7 p=0.0218; Day9 p=0.0213; Day11 p=0.0086; Day13 p=0.0290; Day15 p=0.0285 D1Gi vs D1WT: Day1 p=0.0299; Day17 p=0.0187 ; Day19 p=0.0703; Day21 p=0.0174; Day25 p=0.0223; Day27 p=0.0770; Day29 p=0.0090; Day31 p=0.0325; Day33 p=0.0808
Figure 5G	One way ANOVA	D1 WT = 12 D1 GI = 11 D1 Gq = 12	Weight variation following CNO period	F(2, 32)=4.039 P=0.0273 Bonferroni's multiple comparisons test: D1Gi vs D1Gq p=0.0220
Figure 5G	One way ANOVA	D1 WT = 12 D1 GI = 11 D1 Gq = 12	Fat mass variation following CNO period	F(2, 32)=3.492 P=0.0425 Bonferroni's multiple comparisons test: D1Gi vs D1Gq p=0.0463
Figure 5G	One way ANOVA	D1 WT = 12 D1 GI = 11 D1 Gq = 11 1 outlier value removed with Grubbs' method (Alpha = 0.01)	Weight variation following CNO withdrawal	F(2, 31)=5.789 P=0.0073 Bonferroni's multiple comparisons test: D1Gi vs D1Gq p=0.0063
Figure 5G	Kruskal-Wallis test	D1 WT = 12 D1 GI = 10 D1 Gq = 11 2 outlier values removed with Grubbs' method (Alpha = 0.01)	Fat mass variation following CNO withdrawal	Kruskal-Wallis statistic: 9.225 ; P=0.0099 Dunn's multiple comparisons test D1WT vs D1Gq p=0.0139 D1Gi vs D1Gq p=0.0544
Figure 6				
Figure 6B	Mixed-effects model (Geisser-Greenhouse's epsilon correction)	D1-D2 WT = 11 D1Gq-D2Gi = 8 D1Gi-D2Gq = 11	High fat consumption D1-9 ; D24-25	Time effect F(4.272, 115.3)=32.84 P<0.0001 (ε correction : 0.6103) Virus effect F(2, 27)=0.3648 P=0.6977 Interaction F(14.189)=7.911, P<0.0001 Bonferroni's multiple comparisons test: WT vs D1GqD2Gi: Day1 p=0.0498; Day24 p=0.0056; Day25 p=0.0769 WT vs D1GiD2Gq: Day3 p=0.0648; Day24 p=0.0967 D1GiD2Gq vs D1GqD2Gi: Day1 p=0.0057; Day3 p=0.0277; Day24 p=0.0004; Day25 p=0.0001
Figure 6B	One way ANOVA	D1-D2 WT = 11 D1Gq-D2Gi = 8 D1Gi-D2Gq = 11	High fat consumption mean D10-22	F(2, 27)=1.880 P=0.1720
Figure 6B	One way ANOVA	D1-D2 WT = 11 D1Gq-D2Gi = 8 D1Gi-D2Gq = 11	High fat consumption mean D26-33	F(2, 27)=1.425 P=0.2580

Figure 6C	Mixed-effects model (Geisser-Greenhouse's epsilon correction)	D1-D2 WT = 9 D1Gq-D2Gi = 8 D1Gi-D2Gq = 9 (2 WT and 2 D1Gq-D2Gi animals were exposed to a running wheel without recording) 6 outlier values removed with Grubbs' method (Alpha = 0.01)	Running wheel variation	Time effect F(2.425, 53.64)=2.841 P=0.0573 (ε correction : 0.1427) Virus effect F(2, 23)=8.839 P=0.0014 Interaction F(34.376)=3.486 P<0.0001 Bonferroni's multiple comparisons test: WT vs D1Gq-D2Gi: Day1 p=0.0791; Day3 p=0.0122; Day5 p=0.0013; Day7 p=0.0148; Day9 p=0.0105; Day13 p=0.0106; Day15 p=0.0164; Day17 p=0.0059; Day19 p=0.0010 D1Gi-D2Gq vs WT: Day1 p=0.0966; Day3 p=0.0600; Day5 p=0.0005; Day11 p=0.0336; Day13 p=0.0039; Day15 p=0.0331; Day17 p=0.0047; Day19 p=0.0282; Day21 p=0.0568; Day23 p=0.0443
Figure 6D	One way ANOVA	D1-D2 WT = 11 D1Gq-D2Gi = 8 D1Gi-D2Gq = 11	Weight variation (D1-D23)	F(2, 27)=9.421 P=0.0008 Bonferroni's multiple comparisons test: WT vs D1Gi-D2Gq: p=0.0638 D1Gq-D2Gi vs D1Gi-D2Gq p=0.0006
Figure 6D	Kruskal-Wallis test	D1-D2 WT = 11 D1Gq-D2Gi = 7 D1Gi-D2Gq = 11 1 outliers value removed with Grubbs' method (Alpha = 0.01)	Fat mass variation (D1-D23)	Kruskal-Wallis statistic: 16.74 P=0.0002 Dunn's multiple comparisons test WT vs D1Gq-D2Gi p=0.0408 D1Gq-D2G vs D1Gi-D2Gq p<0.0001
Figure 6D	One way ANOVA	D1-D2 WT = 11 D1Gq-D2Gi = 8 D1Gi-D2Gq = 11	Weight variation (D23-D36)	F(2, 27)=19.79 P<0.0001 Bonferroni's multiple comparisons test: WT vs D1Gi-D2Gq p=0.0004 D1Gq-D2Gi vs D1Gi-D2Gq p<0.0001
Figure 6D	One way ANOVA	D1-D2 WT = 11 D1Gq-D2Gi = 8 D1Gi-D2Gq = 11	Fat mass variation (D23-D36)	F(2, 27)=52.97 P<0.0001 Bonferroni's multiple comparisons test: WT vs D1Gi-D2Gq p=0.0171 WT vs D1Gq-D2Gi p<0.0001 D1Gq-D2Gi vs, D1Gi-D2Gq p<0.0001
Figure 6E	Mixed-effects model (Geisser-Greenhouse's epsilon correction)	D1-D2 WT = 11 D1Gq-D2Gi = 8 D1Gi-D2Gq = 11	Weight variation (Food restricted procedure)	Time effect F(1.421, 38.36)=348.2 P<0.0001 (ε correction : 0.2368) Virus effect F(2, 27)=4.600 P=0.0191 Interaction F(12, 162)=10.63 P<0.0001 Bonferroni's multiple comparisons test: WT vs, D1Gq-D2Gi : 1.5g(Day5) p=0.0467; 1.5g(Day6) p=0.0212
Figure 6E	Mixed-effects model (Geisser-Greenhouse's epsilon correction)	D1-D2 WT = 9 D1Gq-D2Gi = 8 D1Gi-D2Gq = 9 (2 WT and 2 D1Gq-D2Gi animals were exposed to a running wheel without recording) 1 outlier value removed with Grubbs' method (Alpha = 0.01)	Running wheel variation (Food restricted procedure)	Time effect F(3.503, 79.39)=1.644 P=0.1784 (ε correction : 0.5838) Virus effect F(2, 23)=7.484 P=0.0031 Interaction F(12, 136)=5.156 P<0.0001 Bonferroni's multiple comparisons test: WT vs D1Gq-D2Gi: 3g p=0.0027 ; 2.5g p=0.0085 ; 2g p=0.0429 ; 1.5(1) p=0.0318 ; 1.5(3) p=0.0648

Supplementary figure				
Supplementary Figure 2				
Figure Supp 2A	Mixed-effects model (Geisser-Greenhouse's epsilon correction)	D2 GI = 9 D2 Gq = 7	Lever press (Learning)	Time effect F(1.121, 8.972)=139.2, P<0.0001 (ε correction : 0.3738) lever effect F(1.545, 12.36)=177.2 P<0.0001 (ε correction : 0.5151) Interaction F(1.299, 7.508)=46.80 P<0.0001 (ε correction : 0.1444) Bonferroni's multiple comparisons test: Reinforced Lever (L1): D1 Gi vs D1 Gq p=0.7850 Non reinforced Lever (L2): D1 Gi vs D1 Gq p=0.5598
Figure Supp 2B	Two-way RM ANOVA	D2 cre mice: Dreadd Gi = 8 Dreadd Gq= 7	Lick/burst	Virus effect F(1.13)=0.04570 P=0.8340 CNO effect F(1.13)=6.896 P=0.0209 Interaction F(1.13)=0.03268 P=0.8593
Figure Supp 2C	Two-way RM ANOVA	D2 GI =8 D2 Gq = 7	RPM	Virus effect F(1, 13)=1.871 P=0.1946 CNO effect F(1, 13)=1.976 P=0.1833 Interaction F(1, 13)=0.3563 P=0.5608
Figure Supp 2D	Mixed-effects model (Geisser-Greenhouse's epsilon correction)	D1 GI = 9 D1 Gq = 8	Lever press (Learning)	Time effect F(1.104, 8.833)=103.7 P<0.0001 (ε correction : 0.3680) lever effect F(1.555, 12.44)=110.4 P<0.0001 (ε correction : 0.5184) Interaction F(1.925, 13.69)=45.22 P<0.0001 (ε correction : 0.2139) Bonferroni's multiple comparisons test: Reinforced Lever (L1): D1 Gi vs D1 Gq p=0.3512 Non reinforced Lever (L2): D1 Gi vs D1 Gq p>0.9999
Figure Supp 2E	Two-way RM ANOVA	D1 GI = 9 D1 Gq = 8	Lever presses CNO (2mg/kg)	Virus effect F(1.15)=11.59 P=0.0039 CNO effect F(1.15)=13.59 P=0.0022 Interaction F(1.15)=0.3135 P=0.5838
Figure Supp 2E	Two-way RM ANOVA	D1 GI = 9 D1 Gq = 8	Break point CNO (2mg/kg)	Virus effect F(1.15)=9.109 P=0.0086 CNO effect F(1.15)=17.29 P=0.0008 Interaction F(1.15)=0.002770 P=0.9587
Figure Supp 2F	Log-rank (Mantel-Cox) test	D1 GI = 9	Survival Curve CNO (2mg/kg)	DREADD Gi Sal vs CNO: χ2=8.320 ; P Value=0.0039
Figure Supp 2F	Log-rank (Mantel-Cox) test	D1 Gq = 8	Survival Curve CNO (2mg/kg)	DREADD Gq Sal vs CNO χ2=0.154 ; P Value=0.6981
Figure Supp 2G	DREADD Gi : Mixed-effects model (Geisser-Greenhouse's epsilon correction)	D1 Gi = 9	Rate (presses/s) CNO (2mg/kg)	Ratio effect F(2.634, 21.07)=13.85 P<0.0001 (ε correction : 0.3292) CNO effect F(1.000, 8.000)=0.8356 P=0.3874 (ε correction : 1.000) Interaction F(4.193, 32.49)=1.724 P=0.1664 (ε correction : 0.5241)
Figure Supp 2G	DREADD Gq : Mixed-effects model	D1 Gq= 8	Rate (presses/s) CNO (2mg/kg)	Ratio effect F(2.371, 16.60)=4.209 P=0.0281 (ε correction : 0.3534) CNO effect F(1.000, 7.000)=15.63 P=0.0055

	(Geisser-Greenhouse's epsilon correction)			(ε correction : 1.000) Interaction F(2.449, 16.65)=7.832 P=0.0039 (ε correction : 0.2854) Bonferroni's multiple comparisons test: Salin vs CNO : ratio 16, P=0.0757 ; ratio 32, P=0.0165 ; ratio 64, P=0.0139
Figure Supp 2H	Two-way RM ANOVA	D1 Gi = 11 D1 Gq=10	Lick/burst	Virus effect F(1, 19)=3.917 P=0.0625 CNO effect F(1, 19)=2.378 P=0.1395 Interaction F(1, 19)=0.9080 P=0.3526
Figure Supp 2I	Two-way RM ANOVA	D1 Gi = 8 D1 Gq = 8	RPM	Virus effect F(1, 14)=0.04791 P=0.8299 CNO effect F(1, 14)=1.774 P=0.2042 Interaction F(1, 14)=0.05004 P=0.8262
Supplementary Figure 3				
Figure Supp 3A	Mixed-effects model (Geisser-Greenhouse's epsilon correction)	D2 cre mice Dreadd Gi = 7	% Blood glucose change vs baseline	Time effect F(2.576, 15.46)=104.2 P<0.0001 (ε correction : 0.3220) CNO effect F(1.000, 6.000)=1.070 P=0.3409 (ε correction : 1.000) Interaction F(3.077, 18.46)=0.4382 P=0.7330 (ε correction : 0.3846)
Figure Supp 3A	Mixed-effects model (Geisser-Greenhouse's epsilon correction)	D2 cre mice Dreadd Gq = 8	% Blood glucose change vs baseline	Time effect F(1.698, 11.89)=55.82 P<0.0001 (ε correction : 0.2123) CNO effect F(1.000, 7.000)=0.01822 P=0.8964 (ε correction : 1.000) Interaction F(2.704, 18.93)=1.226 P=0.3380 (ε correction : 0.3380)
Figure Supp 3B	Mixed-effects model (Geisser-Greenhouse's epsilon correction)	D1 cre mice Dreadd Gi = 9	% Blood glucose change vs baseline	Time effect F(1.901, 15.21)=74.77 P<0.0001 (ε correction : 0.2376) CNO effect F(1.000, 8.000)=0.1887 P=0.6754 (ε correction : 1.000) Interaction F (2.197, 17.58)=0.3944 P=0.6987 (ε correction : 0.2747)
Figure Supp 3B	Mixed-effects model (Geisser-Greenhouse's epsilon correction)	D1 cre mice Dreadd Gq = 9	% Blood glucose change vs baseline	Time effect F(2.193, 17.54) = 130.8 P<0.0001 (ε correction : 0.2741) CNO effect F(1.000, 8.000) = 2.419 P=0.1585 (ε correction : 1.000) Interaction F(3.290, 26.32) = 1.257 P=0.3601 (ε correction : 0.4113)
Figure Supp 3D	Mixed-effects model (Geisser-Greenhouse's epsilon correction)	D2 cre Dreadd Gi = 7	Fasting refeeding: Chow consumption (1h - 24h) CNO : 2mk/kg	Time effect F(1.652, 9.912)=899.7 P<0.0001 (ε correction : 0.4130) CNO effect F(1.000, 6.000)=15.96 P=0.0072 (ε correction : 1.000) Interaction F(1.969, 11.82)=16.90 P=0.0004 (ε correction : 0.4923) Bonferroni's multiple comparisons test: DREADD GI Sal vs CNO: 1h p=0.0012 ; 2h p=0.0027 ; 4h p=0.0057
Figure Supp 3D	Mixed-effects model	D2 cre Dreadd Gi =7	Fasting refeeding:	Time effect F(1.515, 9.089)=484.6.77 P<0.0001 (ε correction : 0.3787) CNO effect F(1.000, 6.000)=0.1468 P=0.7148 (ε correction : 1.000)

	(Geisser-Greenhouse's epsilon correction)		Chow consumption (1h - 24h) CNO : 0.5mk/kg	Interaction F(1.000, 7.000)=7.520 P=0.0210 Bonferroni's multiple comparisons test: DREADD GI Sal vs CNO: 1h p=0.0280 ; 2h p=0.0099
Figure Supp 3D	Mixed-effects model (Geisser-Greenhouse's epsilon correction)	D2 cre Dreadd Gq = 8	Fasting refeeding: Chow consumption (1h - 24h) CNO : 2mk/kg	Time effect F(1.251, 8.754)=201.0 P<0.0001 (ε correction : 0.3126) CNO effect F(1.000, 7.000)=17.16 P=0.0043 (ε correction : 1.000) Interaction F(1.152, 8.067)=6.396 P=0.00321 (ε correction : 0.2881) Bonferroni's multiple comparisons test: DREADD Gq Sal vs CNO: 12-24h p=0.0370
Figure Supp 3D	Mixed-effects model (Geisser-Greenhouse's epsilon correction)	D2 cre Dreadd Gq = 7 (1 animals excluded)	Fasting refeeding: Chow consumption (1h - 24h) CNO : 0.5mk/kg	Time effect F(1.246, 7.478)=104.9 P<0.0001 (ε correction : 0.3116) CNO effect F(1.000, 6.000)=0.5173 P=0.4990 (ε correction : 1.000) Interaction F(2.218, 13.31)=1.949 P=0.1787 (ε correction : 0.5545)
Figure Supp 3E	Mixed-effects model (Geisser-Greenhouse's epsilon correction	D1 cre Dreadd Gi = 9	Fasting refeeding: Chow consumption (1h - 24h) CNO : 2mk/kg	Time effect F(1.181, 9.451)=414.5 P<0.0001 (ε correction : 0.2953) CNO effect F(1.000, 8.000)=0.3249 P=0.5843 (ε correction : 1.000) Interaction F(2.622, 20.32)=3.468 P=0.0400 (ε correction : 0.6556)
Figure Supp 3E	Mixed-effects model (Geisser-Greenhouse's epsilon correction	D1 cre Dreadd Gi = 8 1 outlier value removed with Grubbs' method (Alpha = 0.01)	Fasting refeeding: Chow consumption (1h - 24h) CNO : 0.5mk/kg	Time effect F(1.309, 9.163)=813.7 P<0.0001 (ε correction : 0.3272) CNO effect F(1.000, 7.000)=9.101P=0.0195 (ε correction : 1.000) Interaction F(1.5658, 10.95)=3.844 P=0.0623 (ε correction : 0.3911) Bonferroni's multiple comparisons test: DREADD Gq Sal vs CNO: 1-24h p>0.9999
Figure Supp 3E	Mixed-effects model (Geisser-Greenhouse's epsilon correction	D1 cre Dreadd Gq = 8 2 outlier values removed with Grubbs' method (Alpha = 0.01)	Fasting refeeding: Chow consumption (1h - 24h) CNO : 2mk/kg	Time effect F(1.407, 9.851)=195.6 P<0.0001 (ε correction : 0.3518) CNO effect F(1.000, 7.000)=16.21 P=0.0050 (ε correction : 1.000) Interaction F(1.548, 10.06)=2.039 P=0.1836 (ε correction : 0.3870)
Figure Supp 3E	Mixed-effects model (Geisser-Greenhouse's epsilon correction	D1 cre Dreadd Gq = 9	Fasting refeeding: Chow consumption (1h - 24h) CNO : 0.5mk/kg	Time effect F(1.938, 15.50)=606.0 P<0.0001 (ε correction : 0.4844) CNO effect F(1.000, 8.000)=14.46 P=0.0052 (ε correction : 1.000) Interaction F(1.642, 13.14)=8.142 P=0.1406 (ε correction : 0.4106) Bonferroni's multiple comparisons test: DREADD Gq Sal vs CNO: 1h p=0.0080 ; 2h p=0.0111 ; 4h p=0.0072

Supplementary Figure 4				
Figure 4A	Mixed-effects model (Geisser-Greenhouse's epsilon correction	D2 cre mice Dreadd Gi = 7	Chow consumption	Time effect F(1.782, 26.72)=15.45 P<0.0001 (ε correction : 0.4454) CNO effect F(1.000, 60.00)=0.5417 P=0.4646 (ε correction : 1.000) Interaction F (1.533, 22.99)=4.968 P=0.0227 (ε correction : 0.3632) Bonferroni's multiple comparisons test: DREADD Gi Sal vs CNO: 3h p=0.0006
Figure 4A	Mixed-effects model (Geisser-Greenhouse's epsilon correction	D2 cre mice Dreadd Gq = 8	Chow consumption	Time effect F(1.922, 13.45)=3.763 P=0.0517 (ε correction : 0.4805) CNO effect F(1.000, 7.000)=2.435 P=0.1626 (ε correction : 1.000) Interaction F (1.647, 11.53)=1.052 P=0.3664 (ε correction : 0.4118)
Figure 4B	Mixed-effects model (Geisser-Greenhouse's epsilon correction	D2 cre mice Dreadd Gi = 7	Wheel running activity	Time effect F(1.894, 11.36)=11.19 P=0.0023 (ε correction : 0.4735) CNO effect F(1.000, 6.000)=17.85 P=0.0055 (ε correction : 1.000) Interaction F(1.582, 9.490)=4.728 P=0.0438 (ε correction : 0.3954) Bonferroni's multiple comparisons test: DREADD Gi Sal vs CNO: 3h p=0.0871 ; 5h p=0.0231
Figure 4B	Mixed-effects model (Geisser-Greenhouse's epsilon correction	D2 cre mice Dreadd Gq = 8 2 outlier values removed with Grubbs' method (Alpha = 0.01)	Wheel running activity	Time effect F(2.084, 14.59)=35.25 P<0.0001 (ε correction : 0.5210) CNO effect F(1.000 , 7.000)=14.38 P=0.0068 (ε correction : 1.000) Interaction F(1.762, 11.45)=9.475 P=0.0045 (ε correction : 0.4404) Bonferroni's multiple comparisons test: DREADD Gq Sal vs CNO: 3h p=0.0011 ; 4h p=0.0726 ;
Figure 4C	Mixed-effects model (Geisser-Greenhouse's epsilon correction	D1 cre Dreadd Gi = 9	Chow consumption	Time effect F(1.856, 14.84)=10.76 P=0.0015 (ε correction : 0.4639) CNO effect F(1.000, 8.000)=1.739 P=0.2238 (ε correction : 1.000) Interaction F(2.506, 20.06)=3.931 P=0.0287 (ε correction : 0.6269) Bonferroni's multiple comparisons test: DREADD Gq Sal vs CNO: 1-24h p>0.9999
Figure 4C	Mixed-effects model (Geisser-Greenhouse's epsilon correction	D1 cre Dreadd Gq = 9 2 outlier values removed with Grubbs' method (Alpha = 0.01)	Chow consumption	Time effect F(2.569, 20.55)=21.55 P<0.0001 (ε correction : 0.6422) CNO effect F(1.000, 8.000)=6.794 P=0.0313 (ε correction : 1.000) Interaction F(2.150, 16.12)=6.184 P=0.0091 (ε correction : 0.5374) Bonferroni's multiple comparisons test: DREADD Gq Sal vs CNO: 3h p=0.0043

Figure 4D	Mixed-effects model (Geisser-Greenhouse's epsilon correction	D1 cre Dreadd Gi = 9 2 outlier values removed with Grubbs' method (Alpha = 0.01)	Wheel running activity	Time effect F(2.393, 19.15)=48.19 P<0.0001 (ε correction : 0.5983) CNO effect F(1.000, 8.000)=2.106 P=0.1848 (ε correction : 1.000) Interaction F(2.518, 18.89)=5.949 P=0.0067 (ε correction : 0.6295) Bonferroni's multiple comparisons test: DREADD Gi Sal vs CNO: 3h p=0.0328
Figure 4D	Mixed-effects model (Geisser-Greenhouse's epsilon correction	D1 cre Dreadd Gq = 9	Wheel running activity	Time effect F(1.858, 14.86)=1.387 P=0.2787 (ε correction : 0.4644) CNO effect F(1.000, 8.000)=12.14 P=0.0083 (ε correction : 1.000) Interaction F(1.420, 11.36)=10.31 P=0.0048 (ε correction : 0.3551) Bonferroni's multiple comparisons test: DREADD Gq Sal vs CNO: 3h p=0.0097 ; 4h p=0.0536 ; 5h p=0.0450
Supplementary Figure 5				
Figure Supp 5B	One way ANOVA	D2 WT = 8 D2 GI = 8 D2 Gq = 9 1 outlier value removed with Grubbs' method (Alpha = 0.01)	Lean mass variation (mean D1-D23)	F(2, 22)=7.281 P=0.0037 Bonferroni's multiple comparisons test: D2 WT vs D2 Gi p=0.0342 D2 WT vs D2 Gq p=0.0039
Figure Supp 5B	One way ANOVA	D2 WT = 9 D2 GI = 8 D2 Gq = 9	Lean mass variation (mean D23-D36)	F(2, 23)=3.737 P=0.0393 Bonferroni's multiple comparisons test: D2 WT vs, D2 Gq p=0.0825
Figure Supp 5E	One way ANOVA	D1 WT = 12 D1 GI = 11 D1 Gq = 12	Lean mass variation (mean D1-D23)	F(2, 32)=2.193 P=0.1280
Figure Supp 5B	One way ANOVA	D1 WT = 12 D1 GI = 11 D1 Gq = 12	Lean mass variation (mean D23-D36)	F(2, 32)=0.7046 P=0.5018
Supplementary Figure 6				
Figure Supp B	One way ANOVA	D1-D2WT= 11 D1Gi-D2Gq = 8 D1Gq-D2Gi = 11	Lean mass variation (mean D1-D23)	F(2, 32)=6.872 P=0.0039 Bonferroni's multiple comparisons test: D1-D2 WT vs D1Gi-D2Gq p=0.0948 D1Gq-D2Gi vs D1Gi-D2Gq p=0.0034
Figure Supp B	One way ANOVA	D1-D2WT= 10 D1Gi-D2Gq = 8 D1Gq-D2Gi = 10 2 outlier values removed with Grubbs' method (Alpha = 0.01)	Lean mass variation (mean D23-D36)	F(2, 25)=15.07 P<0.0001 Bonferroni's multiple comparisons test: D1-D2 WT vs D1Gi-D2Gq p=0.0104 D1Gq-D2Gi vs D1Gi-D2Gq p<0.0001
Figure Supp C	Two-way RM ANOVA	D1-D2WT= 8 D1Gq-D2Gi = 7 D1Gi-D2Gq = 7	Cumulative Chow consumption 2h under leptin or saline	Group effect F(2, 19)=92.61 P<0.0001 Leptin effect F(1, 19)=14.83 P=0.0011 Interaction F(2, 19)=0.8090 P=0.4601

Figure Supp C	Two-way RM ANOVA	D1-D2WT= 8 D1Gq-D2Gi = 7 D1Gi-D2Gq = 7	Cumulative Chow consumption 24h under leptin or saline	Group effect F(2, 19)=19.20 P=0.0543 Leptin effect F(1, 19)=54.72 P<0.0001 Interaction F(2, 19)= 3.410 P<0.0001
Figure Supp D	Mixed-effects model	D1-D2WT= 8 D1Gq-D2Gi = 7 D1Gi-D2Gq = 7 1 outlier value removed with Grubbs' method (Alpha = 0.01)	Cumulative Chow consumption 2h under ghrelin or saline	Group effect F(1, 18)=30.26 P<0.0001 Ghrelin effect F(2, 19)=80.60 P<0.0001 Interaction F(2, 18)= 16.60 P<0.0001 Bonferroni's multiple comparisons test: Saline : D1-D2 WT vs D1Gq-D2Gi p=0.0032 D1-D2 WT vs D1Gi-D2Gq p>0.9999 D1Gq-D2Gi vs D1Gi-D2Gq p=0.0547 Ghrelin : D1-D2 WT vs D1Gq-D2Gi p<0.0001 D1-D2 WT vs D1Gi-D2Gq p=0.0025 D1Gq-D2Gi vs D1Gi-D2Gq p<0.0001
Figure Supp D	Two-way RM ANOVA	D1-D2WT= 8 D1Gq-D2Gi = 7 D1Gi-D2Gq = 7	Cumulative Chow consumption 24h under ghrelin or saline	Group effect F(2, 19)=9.446 P=0.0014 Ghrelin effect F(1, 19)=6.859 P=0.0169 Interaction F(2, 19)= 2.327 P=0.1247

STAR Methods

Experimental models and subject details

Adult male D1-Cre, D2-Cre, D1-Flp-YFP and D1Flp/D2cre (homemade breeding from D1Flp and D2cre mice) mice were used in this study (see table 1 for details). Mice (12 to 28 weeks old) were group housed (4-7 animals), unless otherwise specified, in standard polypropylene cages and maintained in a temperature and humidity controlled environment under a 12:12 light-dark cycle (07:30 on) with *ad libitum* access to water and food. For food consumption experiments, mice were housed in standard polypropylene individual cages. All behavioral procedures were carried out during the light phase unless otherwise specified. Mice were habituated to handling prior to behavioral procedures, and to injection proceeding before test day. All animal care and experimental procedures were in accordance with the INRAE Quality Reference System and to French legislations (Directive87/148, Ministère de l'Agriculture et de la Pêche) and European (Directive 86/609/EEC). They followed ethical protocols approved by the Region Aquitaine Veterinary Services (Direction Départementale de la Protection des Animaux, approval ID: B33-063-920) and by the animal ethic committee of Bordeaux CEEA50. Every effort was made to minimize suffering and reduce the number of animals used.

Stereotaxic viral injections

Mice analgesia was achieved with the subcutaneous injection of buprenorphine (0.05 mg/kg). The animals were then anesthetized using isoflurane (4% induction, 1.5% maintenance) and placed in a stereotaxic frame onto a heating pad. The AAV8-hSyn-DIO-hM4D-mCherry virus (titer of 4.5 x 10^{12} vg/ml l) was used for the Cre-dependent expression of hM4D(Gi) receptor, the AAV8-hSyn-DIO-hM3D-mCherry virus (titer of 5.2 x 10^{12} vg/ml) was used for the Cre-dependent expression of hM3D(Gq) receptors and the AAV8-hSyn-DIO-mCherry virus (1×10^{13} vg/ml) was used for the cre dependent expression of mCherry. The AAV8-hSyn1-dFRT-hM4D(Gi)-mCherry(rev)-dFRT-WPRE-hGHp(A) and AAV8-hSyn1-dFRT-hM3D(Gq)-mCherry(rev)-dFRT-WPRE-hGHp(A), were used for the flp-dependent expression of hM3D(Gq) and hM4D(Gi)-receptors (titer of 4 x 10^{12} vg/ml). A total of 0.5µl of virus solution was injected bilaterally in the nucleus accumbens using a 10µl Hamilton syringe at a rate of 100nl/mn at the following stereotaxic coordinates relative to Bregma (in mm) : AP= +1,7 ; ML= +/- 1,1 ; DV= -4 from the surface of the brain. The syringe was left in place for 5 min before being slowly removed. The skin incision was sutured, postoperative analgesia was prolonged with subcutaneous injections, and mice were place on a heating pad until full recovery from the anesthesia. Behavioral experiments were performed 3 to 4 weeks after the surgeries.

Behavioral Procedures

For all behavioral experiments, mice received CNO (0.5 or 2mg/kg as indicated in the text; see table 2 for details) or 0,9% saline solution intraperitoneal (IP) injections 30 min before the beginning of the test. For the experiments requiring training sessions, there were no injections during these steps. CNO solution (2mg/kg or 0.5mg/kg when mentioned, dissolved in sterile 0.9% saline) was prepared daily and protected from light. For acute CNO treatment experiments, each mouse received either CNO or saline in a counterbalanced manner for within subject analysis, across 2 sessions of each behavioral test at minimum. Experimental designs were randomized regarding genotype, virus type, home-cage and testing chamber.

Operant conditioning

Mice were placed under food deprivation and maintained at 85-90% of their baseline *ad libitum* weight. Fourteen operant chambers (30x40x36 cm, Imetronic Bordeaux), each located into a soundproof and light-attenuating cabinet were used. They consisted of 2 plexiglas panels and 2 PVC panels on top of a metal grid floor, lit by a houselight located at the top of the chamber during sessions. A trough was located on the center of one PVC panel, 4cm above the metal grid, and was surrounded by 2 equally distant retractable metal levers (2x4x1cm). A cue light was located 8.5 cm above each lever. The reinforcer was composed of a 15 µl drop of sweetened condensed milk (3.25 Kcal/g) diluted at 10% in tap water delivered in the trough. Both levers were extended at the beginning of each session, except for pavlovian training. Only one lever was reinforced across all operant procedures and pressing on the non-reinforced lever had no consequence. For each mouce, all of the operant procedures were executed in the same operant chamber. Operant chambers were connected to a computer equipped with POLY Software (Imetronic), which allowed for control of the sessions parameters and recording of the data (number of presses on both levers, number of licks in the full or empty trough).

Pavlovian Training

Three to 4 weeks after AAV injections, animals started pavlovian training. Mice were placed in the operant chamber for 30 min sessions, one session per day, during which a reward – a drop of sweetened condensed milk – was delivered in the trough every minute, associated with the emission of a sound (65 db, 3000 Hz, 200ms) and the illumination of the diode located above the future reinforced lever. The reward had to be consumed by the animal in order for a new reward to be delivered. The learning criterion was set at a mean of 20 rewards earned out of 30, across at least 3 daily consecutive sessions.

Fixed Ratio Training (FR)

When the mice reached the pavlovian training criterion, animals started operant conditioning sessions during which they had to press on the reinforced lever in order to obtain the reward. Reinforced lever presses were signaled by the emission of the sound and the cue light. Operant learning started with daily 1-hour fixed ratio 1 schedule of reinforcement (FR1), during which each reinforced-lever press was rewarded. The learning criterion was set at 100 reward dose earned, across four consecutive sessions.

Random Ratio Training (RR)

Once all the mice completed the operant learning criterion, their ability to press on the reinforced lever in order to receive a reward was increased using random ratio schedules. During the sessions, each lever press on the reinforced lever had a given probability of being reinforced (pRR5=0.2, pRR10=0.1, pRR20=0.05). Animals underwent those 3 different ratio across one-hour sessions, each day, 5 days a week. Moving from one ratio to the next one was achieved once lever response values across two consecutive sessions were stable.

Progressive Ratio Task (PRx2)

The motivational component of operant conditioning was evaluated using a progressive ratio task. During the session, the first reward was delivered after two lever presses on the reinforced lever and the following required amount of lever presses doubled after every reward earned. Session was considered terminated after 1 hour or when animals failed to lever press for three minutes, thus defining the session duration. PRx2 tasks were intercalated by RR20 sessions to prevent operant responding extinction. Mice underwent two PRx2 tasks with IP saline injections for basal performances. Then 4 PRx2 tasks were carried out, during which each mouse received CNO (2 mg/kg or 0.5mg/kg ; IP) or saline IP injection twice. Order of Saline/CNO administration was counterbalanced within groups.

Licking microstructures

A homemade setup was used to record licking microstructures (Ducrocq et al., 2019, 2020). The test was run in polypropylene cages equipped with a feeding bottle and a metal grid floor connected to a computer with a dedicated software. The animal's contact between the grid floor and the metallic sipping tip of the bottle allowed for the precise detection of licks. Mice were habituated to the testing chamber with bottles filled with water for 2 days through 30 min sessions. On the test day, the bottle was filled with 10% condensed sweet milk diluted in tap water and mice were injected with CNO (2 mg/kg) or saline solution 30 min before the beginning of the 30-min testing session. The system allowed the detection of the total number of licks, total number of bursts and number of licks per burst. Bursts were defined as sequences of high frequency licks, in which the interlick interval was less than 250ms. Relation between

number of licks per burst and hedonic reactivity have been demonstrated in (Ducrocq et al., 2020; Johnson, 2018b; Ward et al., 2012).

Motor coordination in rotarod

A rotarod apparatus (Bioseb) was used to assess motor coordination and balance of mice under CNO (2mg/kg). Mice were placed on the rod rotating at 4rpm. During the test, the rotation of the rod increased from 4rpm to 40rpm in 300 sec. The latency to fall was recorded.

Measure of 48-hour ad libitum food intake

Single-housed mice were food deprived for 2 hours and were injected with CNO (2 mg/kg ; IP) 30mn before the onset of the dark phase. Chow pellets were placed in a dish into the cage. Food dishes were weighed after 1 ; 2 ; 4 ; 12 ; 24 and 48 hours. The same test was performed with animal receiving simultaneous CNO (2mg/kg; IP) and leptin infusions (5mg/kg; IP) 3 hours before dark phase, or CNO (2mg/kg; IP) and ghrelin infusions (3mg/kg; IP) at the beginning of the light phase (9.30 AM). In this latter condition, chow pellets were placed in a dish into the cage 30 minute after injections (10.00 AM).

Fasting Refeeding procedure

Single-housed mice previously exposed to high fat diet (Research Diet ref: D12451), were food deprived for 12 hours, then injected with CNO (2 mg/kg or 0.5mg/kg ; IP) 30mn before the onset of the dark phase. Following high fat diet access, food was weighed at 1 ; 2 ; 4 ; 12 ; 24 and 48 hours.

Glucose Tolerance Test

Single-housed mice were food deprived 5 hours prior to the test at 09:00. Glycemia was measured using single-use test strips and glycemia meter (ACCU-CHEK Performa, Roche). The tip of the tail of the animal was cut for the first measurement, in order to obtain 1-2 drops of blood. For the following blood tests, the tail was massaged from the base to the tip so that a small volume of blood comes out. The first drop was wiped away and the second drop was used to measure glycemia. Mice were injected with CNO (2mg/kg ; IP) or saline 20 minutes prior to the beginning of the test. Glucose (2g/kg ; IP) was injected to the mice at t=0mn. Nine blood samples were collected throughout the test (-30mn before CNO/Saline injection; 0mn before glucose injection ; +15mn ; +30mn ; +45mn ; +60mn ; +90mn ; +120mn ; +180mn) and mice were left quiet in a closed soundproof room in between samples.

Effect of acute manipulation of MSNs on wheel-running/free-feeding

The setup consisted of a magnetic fast-track running wheel mounted onto a mouse igloo shelter (BioServ) and connected to a magnet odometer. Single-housed mice had free access to regular chow and the running wheel for 2 days for habituation. On the test day, mice were fasted for 12 hours then placed in the cage with the running wheel and *ad libitum* chow placed inside the cage for 2 hours for baseline consumption and wheel activity. CNO (2 mg/kg) or saline was then injected and food intake and wheel activity were recorded every hour for 3 hours. For each condition (pre- or post infusion), data are expressed as the difference between CNO and saline condition, divided by the value under saline condition. Animals with at least one outlier ratio value (Grubb's method) were excluded from analysis.

Effect of chronic manipulation of MSNs on wheel-running/free-feeding

Single-housed mice were exposed to a running wheel and standard diet for 1 week prior to the beginning of the test. 24-hour wheel running activity, food consumption and weight variation were recorded and defined as a baseline. On the first day of the test animals' food was switched to HFD and CNO (2mg/kg) was administered every day before the onset of the dark period for 23 days, during which variation of percentage of the aforementioned parameters were evaluated. Measurements were pursued for 10 days with no CNO administration. Subsequently, mice were subjected to progressive food restriction over 7 days (decrease of 0.5 g per day, starting at 3g) with a daily CNO infusion and free access to the running wheel.

MRI for body composition

Before and after CNO (2 mg/kg) injection/withdrawal period, total mass tissue including fat mass, fluid mass, and lean mass content were measured using magnetic resonance imaging (EchoMRI, minispec LF90II; Bruker, Wissembourg, France)

Immunohistochemistry

Mice were deeply anesthetized using a lethal IP dose of sodic pentobarbital (Exagon, 300mg/kg) together with lidocaine (Lurocaine 30m g/kg), and transcardially perfused with an ice cold 4% paraformaldehyde solution in PBS 1X. Brains were removed and immersed in 4% PFA overnight at 4°C, then transferred in cryoprotectant solution (30% glycerol ; 30% ethylene glycol in PBS-1X pH 7.4), and stored at -20°C until further use. Brains were rinsed in PBS 1X for 30 min before slicing. 40µm coronal sections were collected using a vibratome (Leica) into cryoprotectant solution and stored at -20°C until further use. Brain slices were mounted on slides and coverslipped with VectaShield containing DAPI mounting medium (Vector Labs). mCherry expression was visualized with a Hamamatsu NANOZOOMER 2.0HT microscope (Bordeaux Imaging Center facilities). For mCherry signal amplification, brain sections were rinsed in PBS-1X, treated with blocking buffer (10% Fetal Bovine Serum in TBS: Tris 0.1M,

NaCl 0.9%, pH 7.4) for 2 h at room temperature (RT) and incubated overnight at 4°C with primary antibody against mCherry (rabbit; 1:1000) and cre recombinase (rabbit; 1:1000). Sections were then incubated with the secondary antibody (donkey anti-rabbit ; 1:5000) conjugated to a fluorophore for 2 hours RT and mounted on slides and coverslipped with VectaShield containing DAPI mounting medium and the signal was visualized with a Hamamatsu NANOZOOMER 2.0HT microscope. To evaluate viral expression in cholinergic interneurons, the procedure was repeated with a primary antibody against ChAt (Choline acetyl transferase; goat ; 1:500) and a secondary antibody (donkey anti-goat ; 1:1000). To evaluate recombinase expression in D1Flp/D2cre mice (D1-MSN : Flippase recombinase and D2-MSN : Cre recombinase), the procedure was repeated with a primary antibody against cre (1:1000) and a secondary antibody (donkey anti-goat ; 1:1000) while YFP signal was used as a reporter of flippase expression.

Ventral tegmental area recordings

Stereotaxic surgery for electrophysiology experiments was performed under isoflurane anesthesia as previously described (Georges and Aston-Jones, 2002). Recording pipettes were inserted into the VTA with the skull flat, at the following coordinates: -3.16mm from bregma; 0.5mm from midline. A glass micropipette (tip diameter=2-3µm, 4-6Mohm) filled with a 2% pontamine sky blue solution in 0.5M sodium acetate was lowered into the VTA. DA neurons were identified according to well-established electrophysiological features (Grace, 1988; Ungless et al., 2004). These included: 1) an half action potential width ≥1.1ms; 2) slow spontaneous firing rate (<10Hz); 3) single and burst spontaneous firing patterns. Through these electrodes, the extracellular potential was recorded with an Axoclamp2B amplifier in the bridge mode. The extracellular potential amplified 10 times by the Axoclamp2B amplifier was further amplified 100 times and filtered (low-pass filter at 300 Hz and high-pass filter at 0.5 kHz) via a differential AC amplifier (model 1700; A-M Systems, Carlsborg, WA). Single neuron spikes were discriminated and digital pulses were collected on-line using a laboratory interface and software (CED 1401, SPIKE 2, Cambridge Electronic Design). Four parameters of VTA DA neuron impulse activity were computed over 200-second epochs after a 5-minute stable baseline period: 1) the basal firing rate, 2) the basal bursting rate, 3) the mean number of spikes per bursts and 4) the number of spontaneously active cells per track. The onset of a burst was defined as the occurrence of two spikes with an interspike interval <80msec (Grace, 1988).

SUPPLEMENTAL INFORMATION

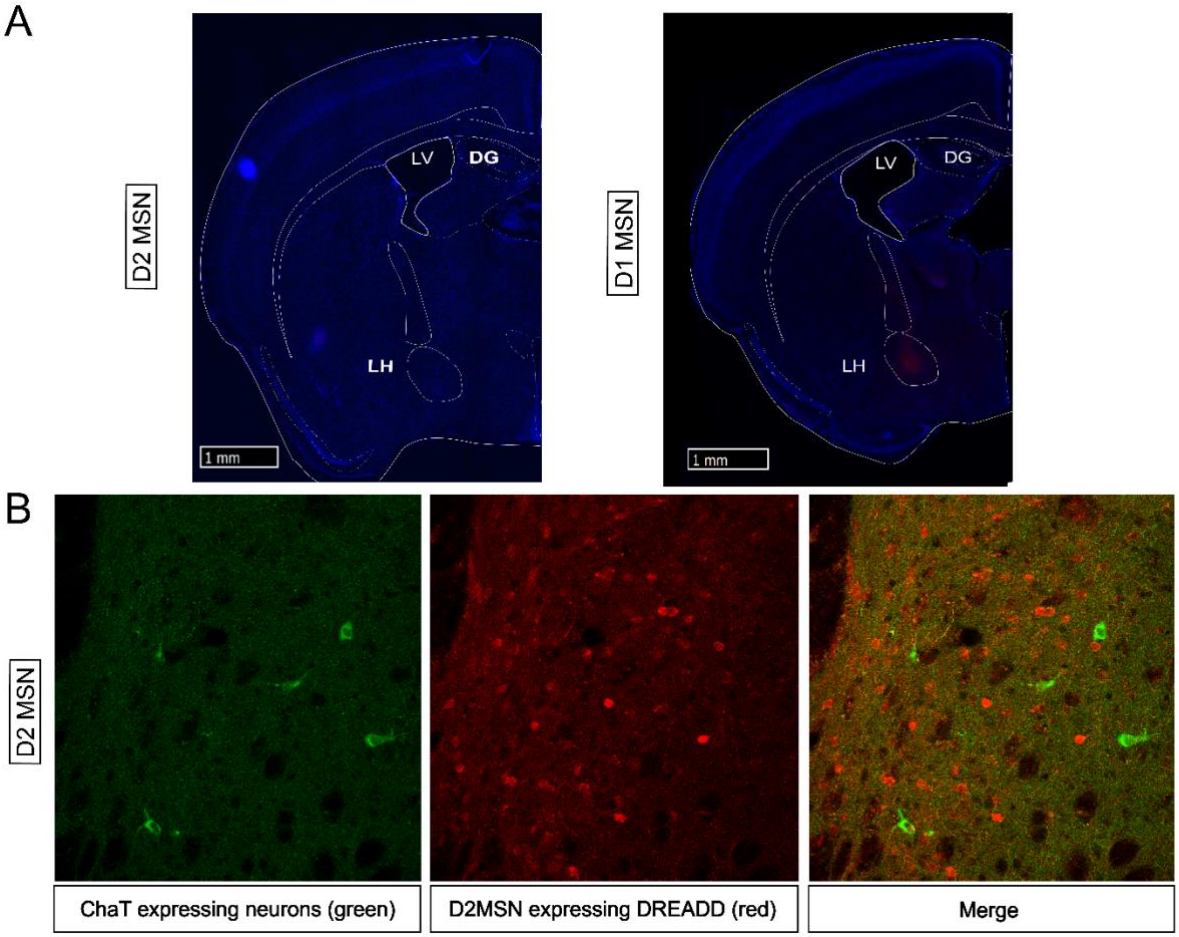

Suppl. Figure 1 (relates to Figure 1): A) Coronal sections of D2-cre (Top, left) and D1-cre (Top right) mouse brains expressing cre-dependent DREADD fused to mCherry in the NAc core. B) Representative picture of NAc coronal section (X40) with immuno-labeled ChAT (Choline acetyl transferase) in green, (Bottom left), immuno-labeled DREADD in red (Bottom middle) and merge (Bottom right) supporting a lack of DREADD expression in cholinergic interneurons. See Table 2 for statistical analyses.

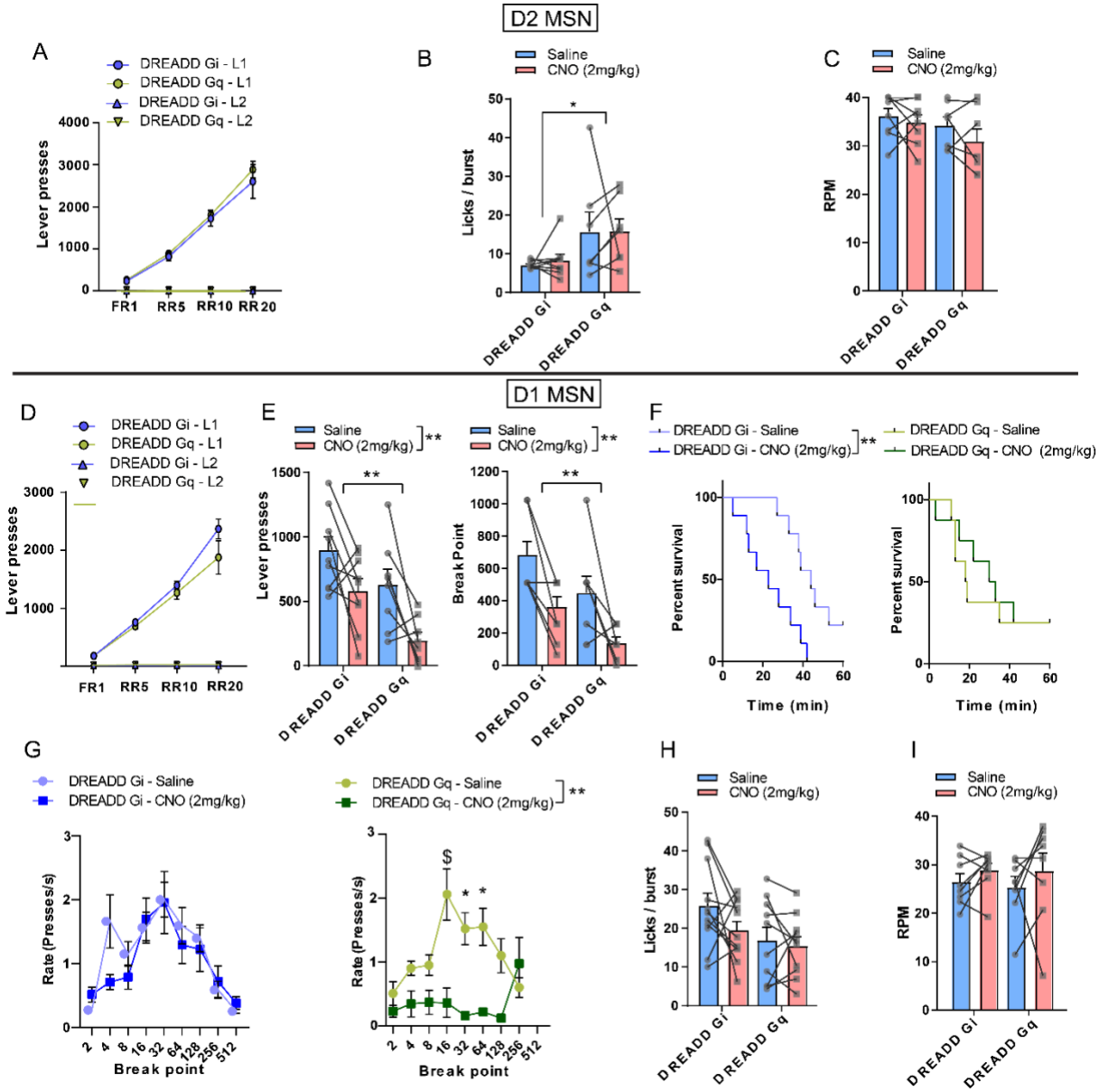

Suppl. Figure 2 (relates to Figure 2):

(A) Number of lever presses on the reinforced (L1) and non-reinforced (L2) levers across the different schedules of reinforcement in D2-cre mice expressing either DREADD Gi or DREADD Gq in the NAc, in the absence of CNO administration. (B) Licking microstructures (number of licks per burst) during consumption of a palatable solution (milk) in D2-cre mice expressing DREADD Gi or Gq. (C) Rotation per min (RPM) in a rotarod in D2-cre mice under inhibition (DREADD Gi) or activation (DREADD Gq) of D2-MSNs. (D) Number of lever presses on the reinforced (L1) and non-reinforced (L2) levers across the different schedules of reinforcement in D1-cre mice expressing either DREADD Gi or DREADD Gq in the NAc, in the absence of CNO administration. (E) Effect of 2 mg/kg CNO in D1-cre mice expressing DREADDs Gi or Gq on the number of lever presses (left), breakpoint (right) and (F) percent survival in the PR task. (G) Rate of lever presses as a function of ratio requirement during the PR task. (H) Licking microstructures (number of licks per burst) during consumption of a palatable solution (milk) under inhibition (DREADD Gi) or activation (DREADD Gq) of D1-MSNs. (I) Rotation per min (RPM) in a rotarod in D1-cre mice under inhibition (DREADD Gi) or activation (DREADD Gq) of D2-MSNs. (CNO: 2mg/kg); D2-cre: DREADD Gi n=9, DREADD Gq n=7; D1-cre: DREADD Gi n=9, DREADD Gq n=8. * : p<0.05 ; ** : p<0.01 ; *** : p<0.001 ; Error bars = s.e.m. See Table 2 for statistical analyses.

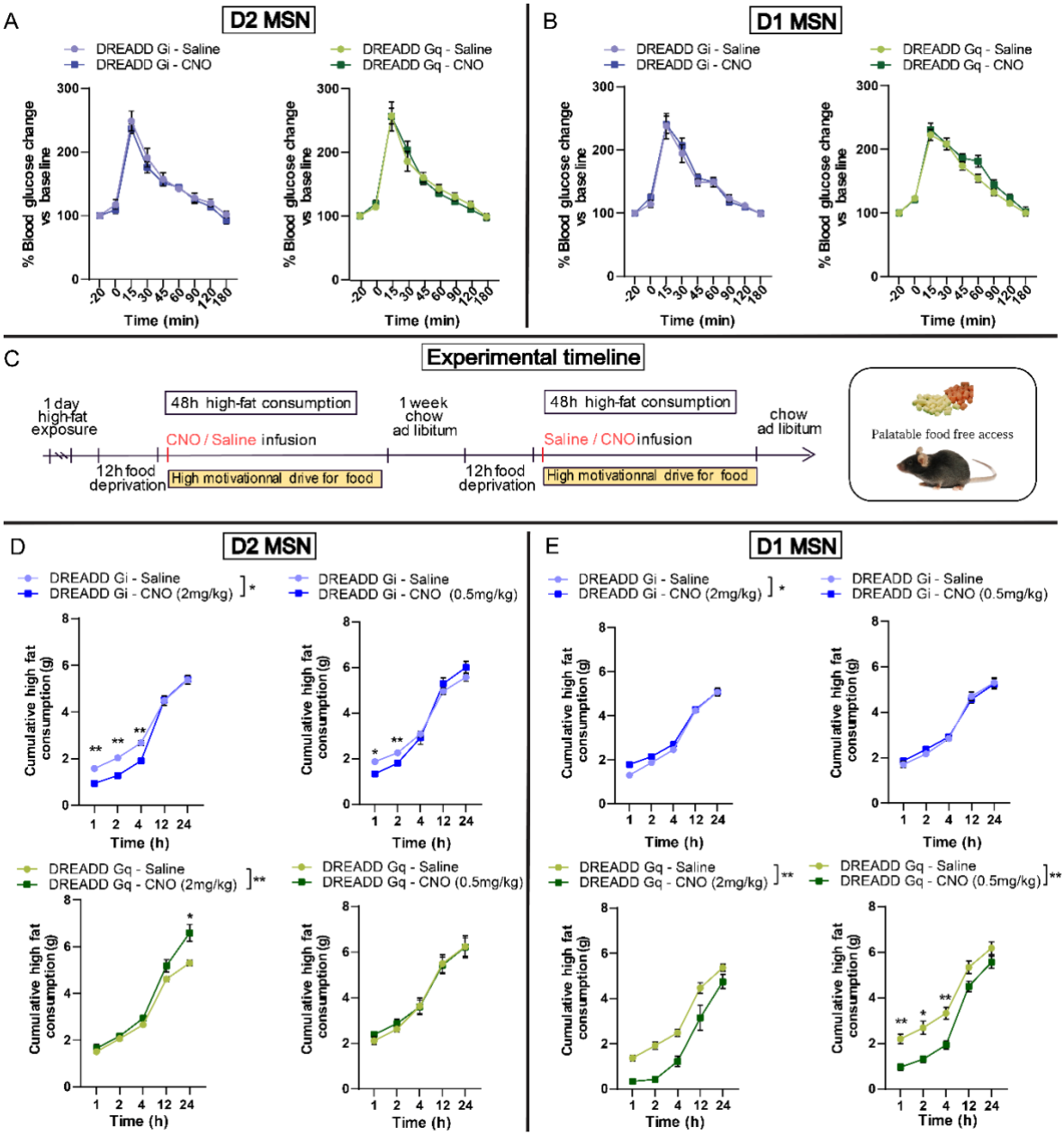

Suppl. Figure 3 (relates to Figure 3):

(A-B) Glucose tolerance test under acute chemogenetic inhibition (DREADD Gi) or activation (DREADD Gq) of NAc D2-MSNs (A) and D1-MSNs (B). **(C)** Experimental design for the fasting-refeeding protocol. **(D-E)** Cumulative high fat consumption in D2-cre (D) and D1-cre (E) mice expressing DREADD Gi (top) or Gq (bottom) under CNO 2mg/kg (left) or 0,5 mg/kg (right). D2-cre: DREADD Gi n=7, DREADD Gq n=8; D1-cre: DREADD Gi n=9, DREADD Gq n=9. * : p<0.05 ; ** : p<0.01 ; *** : p<0.001 ; Error bars = s.e.m**.** See Table 2 for statistical analyses.

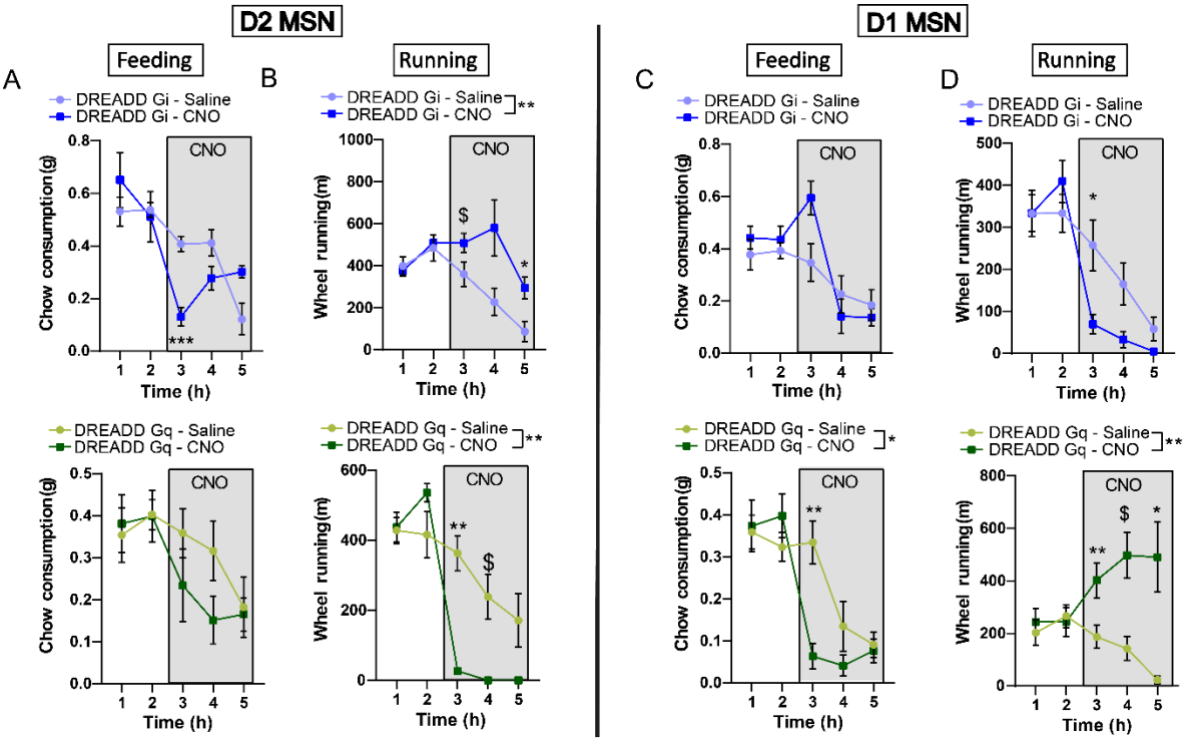

Suppl. Figure 4 (relates to Figure 4):

Chemogenetic-mediated inhibition of D2-MSNs decreases and increases food intake (A, top) and wheel-running (B, top), respectively. D2-MSNs activation spared food intake (A, bottom) but strongly decreased voluntary wheel-running (B, bottom). D1-MSNs inhibition increased food intake (C, top) while decreasing wheel-running (D, top), while their activation decreases and increases food intake (C, bottom) and wheel-running (D, bottom), respectively. (CNO: 2mg/kg); D2-cre: DREADD Gi n=7, DREADD Gq n=8 ; D1-cre: DREADD Gi n=9, DREADD Gq n=9. * : p<0.05 ; ** : p<0.01 ; *** : p<0.001 ; Error bars = s.e.m. See Table 2 for statistical analyses.

A

D2 MSN

Age range	D2 WT (n= 9)			D2 Gi (n= 8)			D2 Gq (n= 9)		
Experimental time	D0	D23	J34	D0	D23	D34	D0	D23	D34
Mean Weight (g)	29,81	31,11	32,74	28,95	30,48	31,66	28,36	30,52	29,96
SEM	±0,38	±0,59	±0,70	± 0,49	± 0,73	± 1,04	± 0,46	± 0,88	± 0,95
Mean Fat (g)	3,97	6,41	7,92	2,55	5,75	6,99	2,69	6,62	5,78
SEM	±0,26	±0,58	±0,63	± 0,27	± 0,69	± 1,07	± 0,41	± 0,78	± 0,85
Mean Lean (g)	20,92	19,38	19,17	21,67	19,54	19,23	20,96	18,67	19,08
SEM	±0,25	±0,23	±0,13	± 0,28	± 0,28	± 0,3	± 0,19	± 0,2	± 0,37
Experimental time	Training	D0 - D23	D23-D34	Training	D0 - D23	D23-D34	Training	D0 - D23	D23-D34
Mean run (m)	4215,76	8341,84	8028,7	5357,93	9900,83	8407,36	6668,95	6002,78	10074,7
SEM	±422,48	±1402,65	±1573,33	±550,96	± 408,57	± 840,72	±918,99	±810,34	±706,13

B

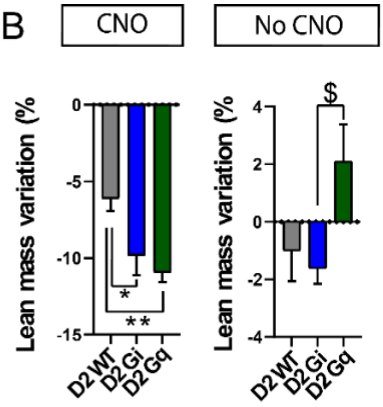

C

D1 MSN

	D1 WT (n= 12)			D1 Gi (n= 11)			D1 Gq (n= 12)		
Experimental time	D0	D23	D50	D0	D23	D50	D0	D23	D50
Mean Weight (g)	29,61	30,18	33,83	27,74	29,81	32,37	28,24	27,95	31,92
SEM	±0,6	±0,71	±0,71	± 0,64	± 1,18	± 1,35	± 0,54	± 0,59	± 0,78
Mean Fat (g)	3,26	5,3	9,09	2,36	6,13	9,79	2,2	3,23	8,07
SEM	±0,34	±0,45	±0,49	± 0,28	± 1,01	± 0,86	± 0,22	± 0,41	± 0,4
Mean Lean (g)	21,59	19,69	18,88	20,96	18,52	17,7	21,45	19,87	19,21
SEM	±0,42	±0,19	±0,19	± 0,38	± 0,32	± 0,29	± 0,35	± 0,35	± 0,29
	Training	D0 - D23	D23-D34	Training	D0 - D23	D23-D34	Training	D0-D23	D23-D34
Mean run (m)	5146	7194	8836	6071	6292	5790	6152	11840	11466
SEM	±473,35	±716,27	±1133,89	±823,95	±1167,71	±1015,17	±606,94	±852,55	±1014,5

D

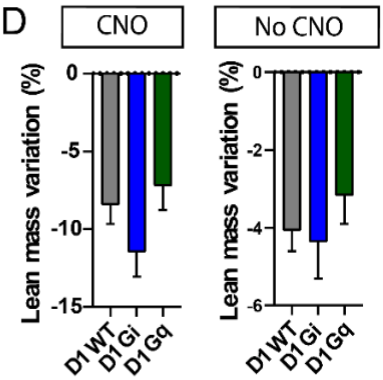

Suppl. Figure 5 (relates to Figure 5):

(A) Table for mass parameters (grams) and running (meters) for chemogenetic manipulations of D2-MSNs. (B) Variation in lean mass at the end of chronic chemogenetic manipulation of D2-MSNs (CNO) and after CNO withdrawal (No CNO). (C) Table for mass parameters (grams) and running (meters) for chemogenetic manipulations of D1-MSNs. (D) Variation in lean mass at the end of chronic chemogenetic manipulation of D2-MSNs (CNO) and after CNO withdrawal (No CNO). (CNO: 2mg/kg); D2- WT n=9 ; D2-Gi n=8, D2-Gq n=9. $: 0.05<p<0.1; * : p<0.05 ; ** : p<0.01; Error bars = s.e.m. / D1-WT n=12 ; D1-Gi n=11, D1-Gq n=12. * : p<0.05 ; ** : p<0.01; Error bars = s.e.m. See Table 2 for statistical analyses.

A

Age range	D1-D2 WT (n= 11)			D1Gq-D2Gi (n= 8)			D1Gi-D2Gq (n= 11)		
Experimental time	D0	D23	D34	D0	D23	D34	D0	D23	D34
Mean Weight (g)	34,94	34,12	36,02	29,05	27,88	30,56	31,32	34,29	33,9
SEM	± 1,099	± 1,338	± 1,572	± 0,8049	± 1,188	± 1,699	± 0,7113	± 1,054	± 1,215
Mean Fat (g)	9,318	10,22	11,55	3,353	3,089	5,383	3,794	9,681	8,418
SEM	± 1,331	± 1,59	± 1,92	± 0,475	± 0,9135	± 1,389	± 0,3189	± 0,9147	± 1,017
Mean Lean (g)	19,88	17,82	18,18	20,87	19,89	19,75	22,32	18,41	19,69
SEM	± 0,8713	± 0,7646	± 0,7788	± 0,5535	± 0,3011	± 0,3383	± 0,8522	± 0,6389	± 0,6024
	Training	D0 - D23	D23-D34	Training	D0 - D23	D23-D34	Training	D0 - D23	D23-D34
Mean run (m)	3608	4174	6077	6090	11836	9216	5453	3384	6827
SEM	± 885,9	± 957,8	± 1734	± 1301	± 1822	± 1933	± 855	± 743,4	± 1352

B

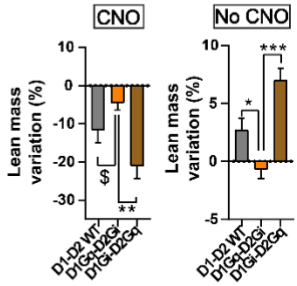

C

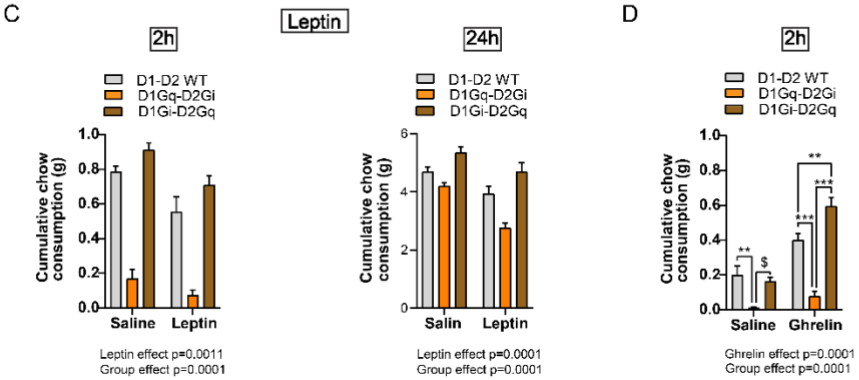

D

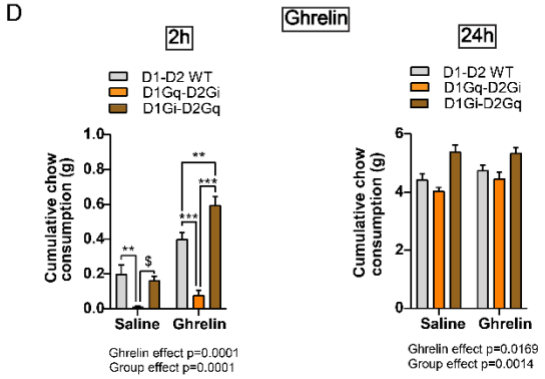

Suppl. Figure 6 (relates to Figure 6):

(A) Table for mass parameters (grams) and running (meters) for chemogenetic concomitant manipulation of D1- and D2-MSNs. (B) Variation in lean mass at the end of chronic simultaneous chemogenetic manipulation of D1- and D2-MSNs (CNO) and after CNO withdrawal (No CNO). (C-D) Standard chow consumption under acute CNO (2mg/kg) together with Ghrelin (3mg/kg) or leptin (5mg/kg) infusions under concomitant chemogenetic manipulation of D1- and D2-MSNs (D1Gq-D2Gi: activation of D1-MSNs together with inhibition of D2-MSNs; D1Gi-D2Gq: inhibition of D1-MSNs together with activation of D2-MSNs; D1-D2 WT: WT animals). D1-D2 WT n=11 ; D1Gi-D2Gq n=11, D1Gq-D2Gi n=8. $: 0.05<p<0.1 * : p<0.05 ; ** : p<0.01; *** : p<0.001 Error bars = s.e.m. See Table 2 for statistical analyses.

REFERENCES

Bailer, U.F., Frank, G.K., Price, J.C., Meltzer, C.C., Becker, C., Mathis, C.A., Wagner, A., Barbarich-Marsteller, N.C., Bloss, C.S., Putnam, K., et al. (2013). Interaction between serotonin transporter and dopamine D2/D3 receptor radioligand measures is associated with harm avoidant symptoms in anorexia and bulimia nervosa. Psychiatry Res *211*, 160–168. https://doi.org/10.1016/j.pscychresns.2012.06.010.

Baimel, C., McGarry, L.M., and Carter, A.G. (2019). The Projection Targets of Medium Spiny Neurons Govern Cocaine-Evoked Synaptic Plasticity in the Nucleus Accumbens. Cell Rep *28*, 2256-2263.e3. https://doi.org/10.1016/j.celrep.2019.07.074.

Baldo, B.A., and Kelley, A.E. (2007). Discrete neurochemical coding of distinguishable motivational processes: insights from nucleus accumbens control of feeding. Psychopharmacology (Berl) *191*, 439–459. https://doi.org/10.1007/s00213-007-0741-z.

Beeler, J.A., Faust, R.P., Turkson, S., Ye, H., and Zhuang, X. (2016). Low Dopamine D2 Receptor Increases Vulnerability to Obesity Via Reduced Physical Activity, Not Increased Appetitive Motivation. Biological Psychiatry *79*, 887–897. https://doi.org/10.1016/j.biopsych.2015.07.009.

Beier, K.T., Steinberg, E.E., DeLoach, K.E., Xie, S., Miyamichi, K., Schwarz, L., Gao, X.J., Kremer, E.J., Malenka, R.C., and Luo, L. (2015). Circuit Architecture of VTA Dopamine Neurons Revealed by Systematic Input-Output Mapping. Cell *162*, 622–634. https://doi.org/10.1016/j.cell.2015.07.015.

Bond, C.W., Trinko, R., Foscue, E., Furman, K., Groman, S.M., Taylor, J.R., and DiLeone, R.J. (2020). Medial Nucleus Accumbens Projections to the Ventral Tegmental Area Control Food Consumption. J Neurosci *40*, 4727–4738. https://doi.org/10.1523/JNEUROSCI.3054-18.2020.

Bonnavion, P., Varin, C., Fakhfouri, G., Groote, A.D., Cornil, A., Isingrini, E., Rainer, Q., Xu, K., Tzavara, E., Vigneault, E., et al. (2022). Unexpected inhibition of motor function by dopamine activation of D1/D2 co-expressing striatal neurons. 2022.04.05.487163. https://doi.org/10.1101/2022.04.05.487163.

Broft, A., Slifstein, M., Osborne, J., Kothari, P., Morim, S., Shingleton, R., Kenney, L., Vallabhajosula, S., Attia, E., Martinez, D., et al. (2015). Striatal dopamine type 2 receptor availability in anorexia nervosa. Psychiatry Res *233*, 380–387. https://doi.org/10.1016/j.pscychresns.2015.06.013.

Bulik-Sullivan, B., Finucane, H.K., Anttila, V., Gusev, A., Day, F.R., Loh, P.-R., ReproGen Consortium, Psychiatric Genomics Consortium, Genetic Consortium for Anorexia Nervosa of the Wellcome Trust Case Control Consortium 3, Duncan, L., et al. (2015). An atlas of genetic correlations across human diseases and traits. Nat Genet *47*, 1236–1241. https://doi.org/10.1038/ng.3406.

Carvalho Poyraz, F., Holzner, E., Bailey, M.R., Meszaros, J., Kenney, L., Kheirbek, M.A., Balsam, P.D., and Kellendonk, C. (2016). Decreasing Striatopallidal Pathway Function Enhances Motivation by Energizing the Initiation of Goal-Directed Action. Journal of Neuroscience *36*, 5988–6001. https://doi.org/10.1523/JNEUROSCI.0444-16.2016.

Casper, R.C. (2006). The “drive for activity” and ‘restlessness’ in anorexia nervosa: potential pathways. J Affect Disord *92*, 99–107. https://doi.org/10.1016/j.jad.2005.12.039.

Casper, R.C. (2018). Not the Function of Eating, but Spontaneous Activity and Energy Expenditure, Reflected in “Restlessness” and a “Drive for Activity” Appear to Be Dysregulated in Anorexia Nervosa: Treatment Implications. Front Psychol *9*, 2303. https://doi.org/10.3389/fpsyg.2018.02303.

Chartoff, E.H., Marck, B.T., Matsumoto, A.M., Dorsa, D.M., and Palmiter, R.D. (2001). Induction of stereotypy in dopamine-deficient mice requires striatal D1 receptor activation. Proc Natl Acad Sci U S A *98*, 10451–10456. https://doi.org/10.1073/pnas.181356498.

Collier, G., and Hirsch, E. (1971). Reinforcing properties of spontaneous activity in the rat. Journal of Comparative and Physiological Psychology *77*, 155–160. https://doi.org/10.1037/h0031588.

Dang, L.C., Samanez-Larkin, G.R., Castrellon, J.J., Perkins, S.F., Cowan, R.L., and Zald, D.H. (2016). Associations between dopamine D2 receptor availability and BMI depend on age. NeuroImage *138*, 176–183. https://doi.org/10.1016/j.neuroimage.2016.05.044.

Ducrocq, F., Hyde, A., Fanet, H., Oummadi, A., Walle, R., De Smedt-Peyrusse, V., Laye, S., Ferreira, G., Trifilieff, P., and Vancassel, S. (2019). Decrease in Operant Responding Under Obesogenic Diet Exposure is not Related to Deficits in Incentive or Hedonic Processes. Obesity *27*, 255–263. https://doi.org/10.1002/oby.22358.

Ducrocq, F., Walle, R., Contini, A., Oummadi, A., Caraballo, B., van der Veldt, S., Boyer, M.-L., Aby, F., Tolentino-Cortez, T., Helbling, J.-C., et al. (2020). Causal Link between n-3 Polyunsaturated Fatty Acid Deficiency and Motivation Deficits. Cell Metab. *31*, 755-772.e7. https://doi.org/10.1016/j.cmet.2020.02.012.

Ekkekakis, P., Vazou, S., Bixby, W.R., and Georgiadis, E. (2016). The mysterious case of the public health guideline that is (almost) entirely ignored: call for a research agenda on the causes of the extreme avoidance of physical activity in obesity. Obes Rev *17*, 313–329. https://doi.org/10.1111/obr.12369.

Floresco, S.B. (2015). The Nucleus Accumbens: An Interface Between Cognition, Emotion, and Action. Annual Review of Psychology *66*, 25–52. https://doi.org/10.1146/annurev-psych-010213-115159.

Frank, G.K.W., Reynolds, J.R., Shott, M.E., Jappe, L., Yang, T.T., Tregellas, J.R., and O'Reilly, R.C. (2012). Anorexia nervosa and obesity are associated with opposite brain reward response. Neuropsychopharmacology *37*, 2031–2046. https://doi.org/10.1038/npp.2012.51.

Friend, D.M., Devarakonda, K., O'Neal, T.J., Skirzewski, M., Papazoglou, I., Kaplan, A.R., Liow, J.-S., Guo, J., Rane, S.G., Rubinstein, M., et al. (2017). Basal Ganglia Dysfunction Contributes to Physical Inactivity in Obesity. Cell Metabolism *25*, 312–321. https://doi.org/10.1016/j.cmet.2016.12.001.

Gaiser, E.C., Gallezot, J.-D., Worhunsky, P.D., Jastreboff, A.M., Pittman, B., Kantrovitz, L., Angarita, G.A., Cosgrove, K.P., Potenza, M.N., Malison, R.T., et al. (2016). Elevated Dopamine D2/3 Receptor Availability in Obese Individuals: A PET Imaging Study with [11C](+)PHNO. Neuropsychopharmacology *41*, 3042–3050. https://doi.org/10.1038/npp.2016.115.

Gallo, E.F., Meszaros, J., Sherman, J.D., Chohan, M.O., Teboul, E., Choi, C.S., Moore, H., Javitch, J.A., and Kellendonk, C. (2018). Accumbens dopamine D2 receptors increase motivation by decreasing inhibitory transmission to the ventral pallidum. Nature Communications *9*. https://doi.org/10.1038/s41467-018-03272-2.

Georges, F., and Aston-Jones, G. (2002). Activation of ventral tegmental area cells by the bed nucleus of the stria terminalis: a novel excitatory amino acid input to midbrain dopamine neurons. J Neurosci *22*, 5173–5187. .

Grace, A.A. (1988). In vivo and in vitro intracellular recordings from rat midbrain dopamine neurons. Ann N Y Acad Sci *537*, 51–76. https://doi.org/10.1111/j.1749-6632.1988.tb42096.x.

Hurel, I., Redon, B., Scocard, A., Malezieux, M., Marsicano, G., and Chaouloff, F. (2019). Beyond the Activity-Based Anorexia Model: Reinforcing Values of Exercise and Feeding Examined in Stressed Adolescent Male and Female Mice. Front Pharmacol *10*, 587. https://doi.org/10.3389/fphar.2019.00587.

Iversen, I.H. (1993). Techniques for establishing schedules with wheel running as reinforcement in rats. J Exp Anal Behav *60*, 219–238. https://doi.org/10.1901/jeab.1993.60-219.

Johnson, A.W. (2018a). Characterizing ingestive behavior through licking microstructure: Underlying neurobiology and its use in the study of obesity in animal models. Int J Dev Neurosci *64*, 38–47. https://doi.org/10.1016/j.ijdevneu.2017.06.012.

Johnson, A.W. (2018b). Characterizing ingestive behavior through licking microstructure: Underlying neurobiology and its use in the study of obesity in animal models. International Journal of Developmental Neuroscience *64*, 38–47. https://doi.org/10.1016/j.ijdevneu.2017.06.012.

Johnson, P.M., and Kenny, P.J. (2010). Dopamine D2 receptors in addiction-like reward dysfunction and compulsive eating in obese rats. Nature Neuroscience *13*, 635–641. https://doi.org/10.1038/nn.2519.

Karlsson, H.K., Tuominen, L., Tuulari, J.J., Hirvonen, J., Parkkola, R., Helin, S., Salminen, P., Nuutila, P., and Nummenmaa, L. (2015). Obesity Is Associated with Decreased -Opioid But Unaltered Dopamine D2 Receptor Availability in the Brain. Journal of Neuroscience *35*, 3959–3965. https://doi.org/10.1523/JNEUROSCI.4744-14.2015.

Kaye, W.H., Wierenga, C.E., Bailer, U.F., Simmons, A.N., Wagner, A., and Bischoff-Grethe, A. (2013). Does a shared neurobiology for foods and drugs of abuse contribute to extremes of food ingestion in anorexia and bulimia nervosa? Biol Psychiatry *73*, 836–842. https://doi.org/10.1016/j.biopsych.2013.01.002.

Kelley, A.E., Baldo, B.A., Pratt, W.E., and Will, M.J. (2005). Corticostriatal-hypothalamic circuitry and food motivation: integration of energy, action and reward. Physiol Behav *86*, 773–795. https://doi.org/10.1016/j.physbeh.2005.08.066.

Klein, D.A., Schebendach, J.E., Gershkovich, M., Bodell, L.P., Foltin, R.W., and Walsh, B.T. (2010). Behavioral assessment of the reinforcing effect of exercise in women with anorexia nervosa: further paradigm development and data. Int J Eat Disord *43*, 611–618. https://doi.org/10.1002/eat.20758.

Krug, I., Villarejo, C., Jiménez-Murcia, S., Perpiñá, C., Vilarrasa, N., Granero, R., Cebolla, A., Botella, C., Montserrat-Gil de Bernabe, M., Penelo, E., et al. (2013). Eating-related environmental factors in underweight eating disorders and obesity: are there common vulnerabilities during childhood and early adolescence? Eur Eat Disord Rev *21*, 202–208. https://doi.org/10.1002/erv.2204.

Kupchik, Y.M., Brown, R.M., Heinsbroek, J.A., Lobo, M.K., Schwartz, D.J., and Kalivas, P.W. (2015). Coding the direct/indirect pathways by D1 and D2 receptors is not valid for accumbens projections. Nature Neuroscience *18*, 1230–1232. https://doi.org/10.1038/nn.4068.

Lowe, M.R. (2020). Weight suppression is a risk factor for eating disorders: Implications for etiology, maintenance, and treatment. Am J Clin Nutr *112*, 907–908. https://doi.org/10.1093/ajcn/nqaa212.

Manwaring, J.L., Green, L., Myerson, J., Strube, M.J., and Wilfley, D.E. (2011). Discounting of Various types of rewards by women with and without binge eating Disorder: Evidence for general rather than specific Differences. Psychol Rec *61*, 561–582. https://doi.org/10.1007/BF03395777.

Matikainen-Ankney, B.A., and Kravitz, A.V. (2018). Persistent effects of obesity: a neuroplasticity hypothesis. Ann N Y Acad Sci *1428*, 221–239. https://doi.org/10.1111/nyas.13665.

Natsubori, A., Tsutsui-Kimura, I., Nishida, H., Bouchekioua, Y., Sekiya, H., Uchigashima, M., Watanabe, M., de Kerchove d'Exaerde, A., Mimura, M., Takata, N., et al. (2017). Ventrolateral Striatal Medium Spiny Neurons Positively Regulate Food-Incentive, Goal-Directed Behavior Independently of D1 and D2 Selectivity. The Journal of Neuroscience *37*, 2723–2733. https://doi.org/10.1523/JNEUROSCI.3377-16.2017.

O'Connor, E.C., Kremer, Y., Lefort, S., Harada, M., Pascoli, V., Rohner, C., and Lüscher, C. (2015). Accumbal D1R Neurons Projecting to Lateral Hypothalamus Authorize Feeding. Neuron *88*, 553–564. https://doi.org/10.1016/j.neuron.2015.09.038.

Pardo-Garcia, T.R., Garcia-Keller, C., Penaloza, T., Richie, C.T., Pickel, J., Hope, B.T., Harvey, B.K., Kalivas, P.W., and Heinsbroek, J.A. (2019). Ventral Pallidum Is the Primary Target for Accumbens D1 Projections Driving Cocaine Seeking. J. Neurosci. *39*, 2041–2051. https://doi.org/10.1523/JNEUROSCI.2822-18.2018.

Presti, M.F., Mikes, H.M., and Lewis, M.H. (2003). Selective blockade of spontaneous motor stereotypy via intrastriatal pharmacological manipulation. Pharmacol Biochem Behav *74*, 833–839. https://doi.org/10.1016/s0091-3057(02)01081-x.

Rizk, M., Mattar, L., Kern, L., Berthoz, S., Duclos, J., Viltart, O., and Godart, N. (2020). Physical Activity in Eating Disorders: A Systematic Review. Nutrients *12*. https://doi.org/10.3390/nu12010183.

Ruegsegger, G.N., and Booth, F.W. (2017). Running from Disease: Molecular Mechanisms Associating Dopamine and Leptin Signaling in the Brain with Physical Inactivity, Obesity, and Type 2 Diabetes. Front Endocrinol (Lausanne) *8*, 109. https://doi.org/10.3389/fendo.2017.00109.

Schebendach, J., Broft, A., Foltin, R.W., and Walsh, B.T. (2013). Can the reinforcing value of food be measured in bulimia nervosa? Appetite *62*, 70–75. https://doi.org/10.1016/j.appet.2012.11.009.

Shroff, H., Reba, L., Thornton, L.M., Tozzi, F., Klump, K.L., Berrettini, W.H., Brandt, H., Crawford, S., Crow, S., Fichter, M.M., et al. (2006). Features associated with excessive exercise in women with eating disorders. Int J Eat Disord *39*, 454–461. https://doi.org/10.1002/eat.20247.

Soares-Cunha, C., Coimbra, B., David-Pereira, A., Borges, S., Pinto, L., Costa, P., Sousa, N., and Rodrigues, A.J. (2016). Activation of D2 dopamine receptor-expressing neurons in the nucleus accumbens increases motivation. Nat Commun *7*, 11829. https://doi.org/10.1038/ncomms11829.

Soares-Cunha, C., Coimbra, B., Domingues, A.V., Vasconcelos, N., Sousa, N., and Rodrigues, A.J. (2018). Nucleus Accumbens Microcircuit Underlying D2-MSN-Driven Increase in Motivation. Eneuro *5*, ENEURO.0386-18.2018. https://doi.org/10.1523/ENEURO.0386-18.2018.

Soares-Cunha, C., de Vasconcelos, N.A.P., Coimbra, B., Domingues, A.V., Silva, J.M., Loureiro-Campos, E., Gaspar, R., Sotiropoulos, I., Sousa, N., and Rodrigues, A.J. (2020). Nucleus accumbens medium spiny neurons subtypes signal both reward and aversion. Mol Psychiatry *25*, 3241–3255. https://doi.org/10.1038/s41380-019-0484-3.

Soares-Cunha, C., Correia, R., Domingues, A.V., Coimbra, B., Vasconcelos, N.A. de, Pinto, L., Sousa, N., and Rodrigues, A.J. (2022). Distinct role of nucleus accumbens D2-MSN projections to ventral pallidum in different phases of motivated behavior. BioRxiv 2020.11.27.401042. https://doi.org/10.1101/2020.11.27.401042.

Steinglass, J.E., Figner, B., Berkowitz, S., Simpson, H.B., Weber, E.U., and Walsh, B.T. (2012). Increased capacity to delay reward in anorexia nervosa. J Int Neuropsychol Soc *18*, 773–780. https://doi.org/10.1017/S1355617712000446.

Taranis, L., and Meyer, C. (2011). Associations between specific components of compulsive exercise and eating-disordered cognitions and behaviors among young women. Int J Eat Disord *44*, 452–458. https://doi.org/10.1002/eat.20838.

Thoeni, S., Loureiro, M., O'Connor, E.C., and Lüscher, C. (2020). Depression of Accumbal to Lateral Hypothalamic Synapses Gates Overeating. Neuron *107*, 158-172.e4. https://doi.org/10.1016/j.neuron.2020.03.029.

Volkow, N.D., Wang, G.-J., Telang, F., Fowler, J.S., Thanos, P.K., Logan, J., Alexoff, D., Ding, Y.-S., Wong, C., Ma, Y., et al. (2008). Low dopamine striatal D2 receptors are associated with prefrontal metabolism in obese subjects: possible contributing factors. Neuroimage *42*, 1537–1543. https://doi.org/10.1016/j.neuroimage.2008.06.002.

Wang, G.J., Volkow, N.D., Logan, J., Pappas, N.R., Wong, C.T., Zhu, W., Netusil, N., and Fowler, J.S. (2001). Brain dopamine and obesity. Lancet *357*, 354–357. .

Ward, R.D., Kellendonk, C., Kandel, E.R., and Balsam, P.D. (2012). Timing as a window on cognition in schizophrenia. Neuropharmacology *62*, 1175–1181. https://doi.org/10.1016/j.neuropharm.2011.04.014.

Watson, H.J., Yilmaz, Z., Thornton, L.M., Hübel, C., Coleman, J.R.I., Gaspar, H.A., Bryois, J., Hinney, A., Leppä, V.M., Mattheisen, M., et al. (2019). Genome-wide association study identifies eight risk loci and implicates metabo-psychiatric origins for anorexia nervosa. Nat Genet *51*, 1207–1214. https://doi.org/10.1038/s41588-019-0439-2.

Weiss, F., Barbuti, M., Carignani, G., Calderone, A., Santini, F., Maremmani, I., and Perugi, G. (2020). Psychiatric Aspects of Obesity: A Narrative Review of Pathophysiology and Psychopathology. J Clin Med *9*. https://doi.org/10.3390/jcm9082344.

Welch, A.C., Zhang, J., Lyu, J., McMurray, M.S., Javitch, J.A., Kellendonk, C., and Dulawa, S.C. (2019). Dopamine D2 receptor overexpression in the nucleus accumbens core induces robust weight loss during scheduled fasting selectively in female mice. Mol. Psychiatry https://doi.org/10.1038/s41380-019-0633-8.

Wierenga, C.E., Bischoff-Grethe, A., Melrose, A.J., Irvine, Z., Torres, L., Bailer, U.F., Simmons, A., Fudge, J.L., McClure, S.M., Ely, A., et al. (2015). Hunger does not motivate reward in women remitted from anorexia nervosa. Biol Psychiatry *77*, 642–652. https://doi.org/10.1016/j.biopsych.2014.09.024.

Wildes, J.E., and Marcus, M.D. (2015). Application of the Research Domain Criteria (RDoC) framework to eating disorders: emerging concepts and research. Curr Psychiatry Rep *17*, 30. https://doi.org/10.1007/s11920-015-0572-2.

Zhu, X., Ottenheimer, D., and DiLeone, R.J. (2016). Activity of D1/2 Receptor Expressing Neurons in the Nucleus Accumbens Regulates Running, Locomotion, and Food Intake. Front Behav Neurosci *10*. https://doi.org/10.3389/fnbeh.2016.00066.